Propagation pathways of classical Labrador Sea Water from its source region to 26°N

Erik van Sebille[1,4], Molly O. Baringer[2], William E. Johns[1], Christopher S. Meinen[2], Lisa M. Beal[1], M. Femke de Jong[3], and Hendrik M. van Aken[3]

Erik van Sebille, Climate Change Research Centre, University of New South Wales Sydney, NSW, Australia, 2052 (E.vanSebille@unsw.edu.au)

[1]Rosenstiel School of Marine and Atmospheric Science, University of Miami, Miami, Florida, USA

[2]Atlantic Oceanographic and Meteorological Laboratory, Miami, Florida, USA

[3]Royal Netherlands Institute for Sea Research, Den Burg, Netherlands

[4]Now at the Climate Change Research Centre (CCRC), University of New South Wales, Sydney, Australia

Abstract. More than two decades of hydrography on the Abaco line east of the Bahamas at 26°N reveals decadal variability in the salinity of classical Labrador Sea Water (cLSW), despite the long distance from its source region in the North Atlantic Ocean. Hydrographic time series from the Labrador Sea and from the Abaco line show a pronounced step-like decrease in salinity; between 1985 and 1995 in the Labrador Sea and between 1995 and 2010 at the Abaco line, suggesting a time lag between the two locations of approximately 9 years. The amplitude of the anomaly at the Abaco line is 50% of the amplitude in the Labrador Sea. A similar time lag and reduction of amplitude is found in the high-resolution OFES model, in which salinity anomalies can be observed propagating through the Deep Western Boundary Current as well as through a broad interior pathway. On its way south to the Abaco line, the cLSW becomes 8 standard deviations saltier due to isopycnal mixing with Mediterranean Outflow Water (MOW). Climatological data in the North Atlantic suggests that the mixing ratio of MOW to cLSW at the Abaco line is 1:4 and that no variability in MOW is required to explain the observed variability at the Abaco line. The data studied here suggest that decadal cLSW anomalies stay relatively coherent while getting advected, despite the important role of interior pathways.

1. Introduction

North Atlantic Deep Water (NADW) is formed in the high-latitude regions of the Atlantic Ocean and incorporates upper Labrador Sea Water (uLSW), classical Labrador Sea Water (cLSW), Iceland-Scotland Overflow Water (ISOW), and Denmark Straits Overflow Water (DSOW). These four water masses can be found at depths below 1000 m throughout most of the Atlantic basin [e.g. Pickart, 1992; Curry et al., 2003], and they make up the bulk of the waters carried by the southward-flowing lower limb of the Atlantic meridional overturning circulation (AMOC). Despite numerous studies over the past few decades, the pathways and time scales associated with the equatorward spreading of NADW are not yet completely resolved.

The southward flow of NADW constitutes most of the return flow of the AMOC. Knowledge of the NADW advection time scale can therefore aid in understanding how and on what time scales changes in deep water formation can be observed downstream, at for example the RAPID/MOCHA array at 26°N [Cunningham et al., 2007]. Apart from increasing the understanding of the North Atlantic deep circulation, the extent to which variability in deep water formation gets smeared out by interior pathways can thus help in interpreting the time series from this array.

Historically, the Deep Western Boundary Current (DWBC) has been perceived as the major advective pathway from the northern to the southern Atlantic Ocean [Fine and Molinari, 1988; Dickson and Brown, 1994]. However, for many years the importance of interior (re)circulation patterns in the advection of NADW has been known [e.g. Worthington, 1976; McCartney, 1992] but poorly observed. Recently, Bower et al. [2009]

suggested that much of the water in the subpolar DWBC is expelled at Flemish Cap and upstream of the Tail of the Grand Banks and subsequently re-entrained into the DWBC before it reaches the subtropics. The experiment by Bower et al. [2009], using isobaric subsurface floats in combination with numerical modelling, confirmed that there is not one pathway to the subtropical Atlantic via the DWBC, but a multitude of pathways involving diversions through the interior. The expulsion of NADW from the DWBC into the interior subtropical North Atlantic was also found by Zhang [2010] in a climate model. Gary et al. [2011] used Lagrangian trajectories in a suite of high-resolution models to investigate the transport in interior pathways and to show that the potential vorticity carried by eddies breaking off the DWBC sustains the deep recirculation gyres in the western subtropical Atlantic.

NADW properties vary over decadal time scales [e.g. Molinari et al., 1998; Dickson et al., 1996; Curry and McCartney, 2001; Rhein et al., 2002; Henry-Edwards and Tomczak, 2006; Kieke et al., 2006; Yashayaev, 2007; Yashayaev et al., 2007a , 2007b; Sarafanov et al., 2009; Fischer et al., 2010]. As the NADW gets advected southward, eddy mixing dilutes the signal of variability, especially as the number of possible pathways between the Northern Atlantic Ocean and any point farther south increases. This means that a 'leaky' DWBC, with enhanced eddy mixing and a larger role for interior pathways as Bower et al. [2009] showed, might be expected to lead to a less pronounced signal of decadal variability away from the regions of deep water formation.

The role of mixing with the interior in increasing the time lag and smearing out variability was studied by Waugh and Hall [2005]. These authors could replicate observed tracer properties in the subpolar North Atlantic Ocean within a simple advective-diffusive

model by assuming that the DWBC is leaky. The interior basin acts in their model as a reservoir where water can be stored for some time before getting re-entrained into the DWBC, increasing the range of time scales between two points along the DWBC. The resulting wide variety of time scales smears out anomalies from the deep water formation region and their model predicts that the amplitude of the anomaly downstream is typically 2% of the original. Hence, anomalies would be virtually undetectable over distances of more than a few thousand kilometers. However, in the real ocean Curry et al. [1998] and Molinari et al. [1998] found a strong correlation between variability in the formation rates of NADW and variability in water properties farther downstream at Bermuda (with a 5 year lag) and the Bahamas (with a 10 year lag), respectively. Waugh and Hall [2005] acknowledged that their model could not explain the relatively strong and coherent signals found in these observational studies. It thus appears that properties move from their source regions using direct and indirect pathways that somehow largely preserve the shape of temporal anomalies.

There is another source water mass at similar densities in the Atlantic Ocean that can influence cLSW property anomalies [e.g. Paillet et al. 1998]. Mediterranean Outflow Water (MOW), formed when Mediterranean Water mixes with water in the Gulf of Cádiz, occupies approximately the same density classes as Labrador Sea Water, but is warmer and more saline [Baringer and Price, 1997; Iorga and Lozier, 1999; Candela, 2001]. Using hydrographic data, Potter and Lozier [2004] and Leadbetter et al. [2007] found significant variability in properties of the MOW. In spreading westward across the basin, the variability in MOW properties might be expected to influence water mass properties at the Abaco line, in addition to the effect of cLSW variability. Quantification of the amount of

MOW mixed into the DWBC at the Abaco line can give an estimate of the importance of this two-source mixing effect.

In this study, we investigate the relationship between decadal variability in the northern and in the subtropical Atlantic Ocean by using hydrographic time series at the Abaco line, a repeat hydrographic section east of Abaco Island in the Bahamas at 26°N, and in the Labrador Sea (Fig 1), as well as climatological atlases and numerical models. The focus is on classical Labrador Sea Water (cLSW), the class of NADW that is formed through deep convection in the Labrador Sea, defined as water within the density range $36.82 \leq \sigma_2 \leq 36.97$ kg/m^3 (see also section 2). Studying water mass properties in the core of this layer, Molinari et al. [1998] found that salinity anomalies get advected from the Labrador Sea to the Abaco line in approximately 10 years. Using repeat hydrography south of Cape Cod, Joyce et al. [2005] measured a typical velocity of cLSW in the DWBC of at least 4 cm/s, in agreement with typical velocities in numerical models (Fig 1). These velocities yield average transit time estimates of only 4 years for the 5000 km between the two locations. This discrepancy between direct advective time scales and observed lags could be explained by the slow interior pathways described by Bower et al. [2009]. The focus of this study is thus how and on what time scales variability in water mass properties propagate through the North Atlantic.

2. Data and Methods

2.1. Hydrographic and climatological data

The Abaco line hydrography forms the primary data set for this study [Fine and Molinari, 1988; Lee et al., 1990; Molinari et al., 1992]. This data set is a collection of 34 hydrographic sections at 26.5°N and between 78°W and 76°W (some sections extend out

to 69.5°W) east of Abaco Island in the Bahamas, collected between 1985 and 2010. Over the years, the zonal resolution (around 25 km) and offshore extent are somewhat variable and the temporal resolution differs greatly, including a three-year gap between March 1998 and April 2001. The first decade of data has been used in multiple studies of the DWBC [Hacker et al., 1996; Vaughan and Molinari, 1997; Molinari et al., 1998]. More recent studies have used these hydrographic data in combination with the moored current meters and pressure-equipped inverted echo sounders which have been deployed near the line since the late 1980s [Lee et al., 1996; Meinen et al., 2004; Johns et al., 2005; Bryden et al., 2005; Meinen et al., 2006; Cunningham et al., 2007].

Molinari et al. [1998] analysed the 1985–1997 Abaco line data set and found a freshening in the cLSW carried by the DWBC around the year 1994, with the freshening seen first closest to the coast. They linked this freshening to changes in the formation rate of cLSW in the Labrador Sea. An extension of their analysis to March 2010 (Fig 2) shows that the water at the $\sigma_{1.5} = 34.67$ kg/m^3 isopycnal in the middle of the cLSW layer (as used in Molinari's study) is still much fresher than in the 1980s. The mean salinity along this isopycnal, within 100 km offshore of the Abaco coast, is 34.989 with a standard deviation of 0.005 between 1985 and 1994, while after 1996 the mean salinity has decreased to 34.966 with the same standard deviation. The 1994–1996 event thus constitutes a drop in salinity of more than 4 standard deviations.

In order to investigate how this variability in the DWBC at the Abaco line is related to its source region, a time series of temperature and salinity in the Labrador Sea compiled by Van Aken et al. [2011] is used. This data set is similar to the time series by Yashayaev

[2007]. The time series is based on a composite of annual surveys (often obtained in summer) through the central Labrador Sea.

For an assessment of the time-mean salinity in the entire North Atlantic, two climatological atlases are used here: the World Ocean Atlas 2005 [WOA05, Boyer et al. 2006] and HydroBase2 [Curry, 1996]. These data sets are based on hydrographic profiles such as the ones at Abaco and the Labrador Sea described above. Both climatologies have a 1° resolution, but they differ in the amount and method of smoothing and interpolation, with HydroBase2 being less smoothed. Fig 8shows that the basin scale patterns of the depth-averaged salinity in the cLSW range in the two climatologies are similar.

2.2. Model data

Hydrographic data in the North Atlantic are unfortunately too sparse in space and time to follow the salinity signals propagating through the basin. Such an analysis of the temporal evolution of salinity in the basin can only be done in numerical models. Four different models are assessed here; three assimilative models and one fully prognostic model. The first model is the 0.5° SODA model [Carton et al., 2000; Carton, 2008], which has 40 levels in the vertical and is based on the POP code. The second model is the DePreSys model [Smith and Murphy, 2007], which has much lower resolution at 1.25° and 20 depth levels. The third model is the Cube84 run of ECCO2 [Marshall et al., 1997; Menemenlis et al., 2005], at a horizontal resolution of 0.25° and 50 depth levels. Since this model relies heavily on satellite altimetry, the model output is available only beginning in 1992. All these models are assimilative and should thus have water mass characteristics similar to the hydrographic data. The fourth and last model used is the OFES model [Sasaki et al., 2008]. At a horizontal resolution of 0.1° and 54 vertical levels the OFES

model has the highest resolution used here. The OFES model is forced with NCEP winds and fluxes, but does not assimilate other data.

2.3. Choosing a density definition

As water circulates through the basin, it mixes and thereby changes its properties. Although diapycnal mixing is much smaller than isopycnal mixing over large time and spatial scales, individual water parcels will experience small changes in their potential density [e.g. McDougall and Jackett 2005]. In part because of this large-scale variability in potential density associated with diapycnal mixing and diffusion, there are several different depth and density definitions in use to describe cLSW.

Fine and Molinari [1988] and Molinari et al. [1992] categorized the water masses at the Abaco line in depth space (instead of density space) using temperature, salinity, oxygen, and CFC properties of the water. According to these two studies, upper Labrador Sea Water (uLSW) at the Abaco line is found between 1000 and 1400 m, classical Labrador Sea Water (cLSW) is found between 1400 and 2300 m, Iceland-Scotland Overflow Water (ISOW) is found between 2300 and 3200 m, and Denmark Strait Overflow Water (DSOW) is found between 3200 and 4500 m. Classification of water masses in the Labrador Sea has been done using at least three different density coordinates: neutral density [γ_n, e.g. Hall et al. 2004], potential density relative to the surface [σ_θ, e.g.][Kieke et al., 2006], and potential density relative to 2000 dbar [σ_2, e.g. Yashayaev 2007].

It should be noted that Yashayaev [2007] does not use one fixed density range to define LSW but rather defines LSW into vintage classes or year classes. Each of these vintage classes is defined by the years it is formed, and the author shows convincingly how different classes have different temperature and salinity properties. The water formed in the early

1990s, for instance, is much denser than the water formed around 2000. Although one could make a case to study the propagation of each of these vintage classes separately, here we use a pragmatic subtropical compilation of several of the Yashayaev [2007] LSW classes. This is done to stay close to the way in which LSW is typically defined outside of the subpolar regions. Moreover, the conclusions from our analysis using the broad cLSW classification also hold for most of the individual σ_2 isopycnals within the cLSW range.

It appears (Fig 3) that the classification in σ_2 space based on the analysis of LSW properties by Yashayaev [2007] agrees best with the local classification in depth space at the Abaco line by Fine and Molinari [1988] and Molinari et al. [1992]. As this study focusses on the Abaco line, we use a regional density classification which most accurately describes the water masses as they are found near the Bahamas. In the rest of this study we calculate all properties on σ_2 coordinates. The cLSW salinity is defined as the depth-averaged salinity between the $\sigma_2 = 36.82$ kg/m^3 and $\sigma_2 = 36.97$ kg/m^3 isopycnals. Using neutral density instead has minor effects on the results and does not change the conclusions. This study focusses mainly on the variability of salinity, and does not deal directly with temperature. However, since all analyses are done in density space, an anomaly in salinity directly translates into a same-sign anomaly in potential temperature (see also Fig 2). Hence, our results also hold for potential temperature anomalies.

3. Results

3.1. Decadal changes in water properties from hydrography

The extension to 2010 (Fig 2) of the original figure by Molinari et al. [1998] is centered on the $\sigma_{1.5} = 34.67$ kg/m^3 isopycnal, corresponding to $\sigma_2 \approx 36.90$ kg/m^3 in the middle of the cLSW layer at approximately 1800 m depth. Here, we expand this analysis to

reveal how the neighbouring water masses changed. Time series of salinity (averaged over the first 100 km offshore of Abaco on σ_2 surfaces) are examined to study how the 1995 freshening affected the entire water column below 800 m. Fig 4shows anomalies with respect to the time mean at each σ_2 surface for all 34 hydrographic sections, while Fig 5(thick lines) shows the water mass properties of each of the 34 hydrographic sections on a TS-diagram. The post-1995 decrease in salinity occurred throughout the entire cLSW layer and in the deeper overflow waters, while salinity anomalies in the uLSW layer after 1996 are mostly positive, although the variability in uLSW salinity is larger than for the other water masses. This larger variability higher in the water column might be related to the effect of deep-reaching eddies impinging on the coast. The freshening event of cLSW and overflow waters is relatively abrupt, occurring within one year between February 1995 and March 1996. Why this event was so abrupt and coherent in depth is unclear, but it is likely not a problem with one particular cruise since it was measured on two separate cruises.

The salinity anomalies in the three deepest water masses vary in concert. This temporal correlation could be related to at least three processes. Firstly, a slow freshening of all water masses at their source would lead to coinciding fresh signals in the Labrador Sea. Dickson et al. [2002] showed that all abyssal waters in the Subpolar North Atlantic (DSOW, ISOW, LSW) had significant decreasing trends in salinity between the 1960s and 2002, which were attributed to a freshening of the Arctic Ocean. Secondly, entrainment between water masses can cause signals to be mixed. For example, as the overflow waters in the Faroe Bank Channel flow down along the topography they encounter cLSW, of which a considerable volume is entrained into the fast flowing, denser overflow waters

[Dickson et al., 2002]. Any change in the properties of cLSW would in this way be mixed into the deeper ISOW layers. However, because of the time lags involved for LSW to arrive in the Iceland Basin and subsequently for the ISOW to advect to the Labrador Sea (both of the order of 5 years, Van Aken et al. [2011]) this process acts mostly on long term trends. Freshening of the source water at the Faroe Bank Channel sill combined with the freshening of the LSW steepened the long term salinity trend in the ISOW found in the Iceland Basin. Thirdly, the occurrence of deep ($>$ 2 km) convection in the Labrador Sea penetrating into the deep layers will mix the signals between density layers associated with LSW and the overflow waters. Yashayaev [2007] showed that in the winter of 1994 mixed layers in the Labrador Sea reached over 2300 m deep, mixing the upper layers of the more saline ISOW into the LSW of that year. This resulted in an increase of the salinity of this LSW class and a decrease of the ISOW salinity underneath the LSW. Of these three processes (variability at the source, entrainment, and mixing through exceptionally deep convection), the latter two would certainly create (just as in the observations, Fig 4) a smaller amplitude of the anomaly in the deeper layers. However, the data sets used in this study are not sufficient to fully separate the relative importance of each of the three processes.

Relating the cLSW salinity at Abaco with that in the Labrador Sea from the data set complied by Van Aken et al. [2011] (Fig 6) shows that the freshening of the entire cLSW layer between 1995 and 2006 at the Abaco line is preceded by a decadal-scale freshening event of cLSW in the Labrador Sea between 1984 and 1995, which is approximately twice as strong as the freshening at the Abaco line. This lag between the two time series suggests an advective time scale between the two locations of approximately 10 years, in agreement

with the result of Molinari et al. [1998] on the $\sigma_2 \approx 36.90$ kg/m^3 isopycnal. When the depth-averaged cLSW salinity for the two hydrographic data sets are spline interpolated to monthly values, there is a maximum positive correlation between the two ($R = 0.80$) at a lag of 9 years. Similar correlations and lags are found for the time series on the individual isopycnals within the cLSW range. None of these correlations, however, is statistically significant at the 90% confidence level. The non-significance is partly due to the trend in Abaco line cLSW salinity, the relatively short time series, and the high variability in the Labrador Sea time series. After 2003, the cLSW salinity at Abaco appeared to rebound consistent with what might be expected after the salinity increase in the Labrador Sea staring in 1995, but this increase was shortlived and a weak down-trend has resumed since 2005. Thus, there is no clear indication yet of a significant increase at Abaco related to the up-trend in salinity in the Labrador Sea beginning in the mid-1990s.

At the Abaco line itself, there is a weak positive correlation between uLSW and cLSW salinity at time scales shorter than two years ($R = 0.43$, which is not significant at the 90% confidence level), while the correlation is weakly negative for time scales longer than five years ($R = -0.45$, also non-significant at the 90% confidence level). These correlations indicate that local dynamics (eddies) on short time scales may cause water properties to vary in concert, while remote thermohaline forcing on longer time scales causes compensation between upper and classical Labrador Sea Water. Compensation between uLSW and cLSW on decadal time scales (partly due to mass conservation) has also been observed in the Labrador Sea, where Kieke et al. [2006] compared layer thickness of the two water masses. At the Abaco line, however, layer thickness does not change

(Fig 7), and hence there is no sign of compensation between the thickness of the two types of Labrador Sea Water.

If water mass changes in the lower limb of the AMOC affect the strength of the overturning, we might expect to see volume transport variations in the DWBC which correlate with the water mass changes. Geostrophic transport within the cLSW layer is related to the slope of the isopycnals in the DWBC. However, long-term changes in transport by broad-scale tilting of isopycnals are hard to measure because of the presence of eddies on individual hydrographic sections. Hence, the slopes of the isopycnals in the Abaco hydrographic sections are too noisy to draw any conclusions on long-term changes in transport associated with the changes in hydrographic properties (not shown). Recently, however, Fischer et al. [2010] used moored current meter data near the Grand Banks at the outflow region of the Labrador Sea to show that there is no trend in transport between 1996 and 2009, although the outflow waters warmed significantly during that period (in agreement with the increase in salinity in the Labrador Sea from 1995 shown in Fig 6). There is thus so far no evidence that the observed decadal variability in DWBC water mass properties is associated with variability in transport at the Abaco line.

Between the Labrador Sea and the Abaco line, the salinity of the cLSW increases significantly, as best illustrated in a temperature-salinity diagram (Fig 5). In the Labrador Sea, the depth-integrated and spline-interpolated cLSW salinity between 1975 and 2000 is on average 34.82 ± 0.02. At the Abaco line, the salinity 10 years later (between 1985 and 2010) is 34.98 ± 0.01, an increase in the mean salinity of 8 times the standard deviation at the Labrador Sea and a decrease in the standard deviation of a factor 2. Note also that because the range in cLSW salinities in the Labrador Sea is more than twice as

large as that at Abaco, the salinity difference between the two locations increases from approximately 0.07 in the 1980s to 0.14 in the 2000s.

These salinity increases are related to isopycnal mixing with high-salinity Mediterranean Overflow Water (MOW). Curry et al. [2003] show an increase in salinity in the eastern subtropical Atlantic, possibly linked to an increase in salinity of the Eastern Mediterranean Deep Waters [Roether et al., 1996], which seems inconsistent with the freshening observed at the Abaco line.

3.2. The role of Mediterranean Outflow Water in climatologies

The mixing of MOW into the DWBC can be studied using the WOA05 and HydroBase2 climatologies, which provide full horizontal coverage of the northern Atlantic Ocean (see also section 2.1). The maps of cLSW layer salinity (left panels in Fig 8) show a tongue of MOW in the subtropical Atlantic Ocean with highest salinities on the eastern side in the Gulf of Cádiz. Due to the influx of high-salinity water in that region, the cLSW salinity in the DWBC increases by more than 0.10 between the Labrador Sea and the Abaco line (right panels of Fig 8). In both climatologies, the salinity along the western Atlantic continental shelf appears to increase approximately linearly from the Grand Banks at 45°N to the Abaco line, suggesting that the influence of MOW builds gradually and nearly uniformly along the current path.

The relative amounts of MOW and cLSW at Abaco can be computed with a simple mixing model [e.g. Beal et al. 2000]. At each σ_2 isopycnal, the mixing fraction of MOW is given by

$$M = \frac{S_{\mathrm{Aba}} - S_{\mathrm{Lab}}}{S_{\mathrm{Med}} - S_{\mathrm{Lab}}} \tag{1}$$

where S_{Aba}, S_{Lab}, and S_{Med} are the salinities at the Abaco line, the Labrador Sea, and the Gulf of Cádiz, respectively. Since the exact locations of water mass formation in the Labrador Sea and in the Gulf of Cádiz are not known, profiles in two rather large regions are used (Fig 1). This yields average values for S_{Lab} and S_{Med} as well as a one standard deviation uncertainty in these values, and this 1σ uncertainty can be used to calculate the standard error in mixing fraction M. Note that this is a lower bound for the uncertainty because by definition it is computed from the already averaged values in the climatology.

Using the HydroBase2 climatology, profiles for each of these regions were constructed by averaging along σ_2 surfaces in the region. Inserting these average profiles into Eq (1) yields a mixing fraction of just above 20% MOW in the cLSW density range, which increases to up to 40% in the uLSW density range (Fig 9b). Using the WOA05 data yields a similar result (not shown).

Apart from isopycnal mixing with MOW, the salinity in the cLSW layer might also increase due to diapycnal mixing. In the Labrador Sea, the maxmimum salinity is attained close to the cLSW–ISOW interface (Fig 5) and the uLSW is much fresher than cLSW, so there can be no increase in salinity from diapycnal mixing with uLSW. In the subtropical gyre, however, the uLSW increases much more in salinity than the cLSW, so there are regions where diapycnal mixing with uLSW can increase the salinity of the cLSW. The order of magnitude of this increase can be estimated by integrating the diapycnal flux $\partial S/\partial t = -K_v \partial^2 S/\partial z^2$ over the 10 years it takes the water to reach the Abaco line. The mean value for $\partial^2 S/\partial z^2$ in the western subtropical North Atlantic on the $\sigma_2 = 36.82$ kg/m^3 interface is $-1 \cdot 10^{-7}$ m^{-2} in the HydroBase2 climatology. Even a high vertical diffusivity parameter of $K_v = 10^{-4}$ m^2/s only yields a ΔS of $3 \cdot 10^{-3}$ when Δt is 10 years.

This is a negligible increase in salinity compared to the observed 0.10 increase of cLSW salinity. Furthermore, cLSW salinity decreases by $3 \cdot 10^{-4}$ due to mixing with ISOW at the lower interface. Hence, it appears that almost all of the increase in salinity is due to isopycnal mixing with MOW.

The mixing fractions from the climatologies can be combined with the hydrographic time series to assess the importance of MOW variability versus cLSW variability. Within the core of the cLSW ($\sigma_2 = 36.90$ kg/m^3, see Fig 9b) the mixing fraction is 21% with a standard error of 4%. Using the hydrographic time series from section 2.1, a mixing ratio as a function of time can be calculated under the assumption of constant MOW salinity. The variability in this time series of mixing ratio can then be compared to the standard error in the climatological mixing ratio, in order to estimate how important variability in MOW is at the Abaco line. The comparison can give an indication of whether one needs to account for MOW variability to explain the observed variability at the Abaco, or whether the variation in M falls within the uncertainty margins.

The mean salinity of the MOW in the cLSW density range is 35.44, which is used as S_{Med} in eq (1), in combination with the Abaco time series for S_{Aba} and the Labrador Sea time series with a lead of 9 years for S_{Lab}. This yields an M with a temporal standard deviation of 2%, which is half of the standard error in mean mixing ratio (the gray area in Fig 9b). The small temporal variability in M for a constant S_{Med} indicates that the variability in the Labrador Sea suffices to explain the variability at the Abaco line. This result is consistent with the high (although not significant) correlation between water mass changes in the Labrador Sea and at Abaco (Fig 6). We thus conclude that the signals of

MOW variability at Abaco are negligible and most water mass changes at the Abaco line are related to changes in the Labrador Sea.

3.3. The skill of models in simulating North Atlantic cLSW salinity

The hydrographic observations in section 3.1 strongly suggest that decadal changes in water mass characteristics formed in the Labrador Sea can be observed as abrupt, coherent changes at Abaco some 5000 km to the south along the western boundary. Yet, Bower et al. [2009] and Gary et al. [2011] show that interior pathways are common, implying a spread of time scales which would smear out abrupt changes. The question is how these two observations add up.

First, to test the skill of the four models described in section 2.2 in simulating the depth-averaged salinity in the cLSW, time series since 1950 (1992 for the ECCO2 model) of all four models are compared to the hydrographic sections at the Abaco line and in the Labrador Sea (Fig 10). Surprisingly, OFES is found to most closely simulate the freshening trend in cLSW at the Abaco line (Fig 10a). The DePreSys model has almost no inter-annual variability and only a very weak freshening in the late 1990s. The ECCO2 model has a freshening around 1995, but then rebounds to early 1990s values by 2005. Finally, the model that agrees least with the hydrography at the Abaco line is SODA, which has unrealistically large decadal variability and shows a large increase in salinity (instead of a decrease) around 2000.

In the Labrador Sea (using the area shown in Fig 1), the interdecadal variation in salinity is captured quite accurately in all models (Fig 10b), although not all of the details of the different year classes [Yashayaev, 2007] are captured to the same extent. The SODA and DePreSys model agree much better with the hydrography in the Labrador Sea than at

the Abaco line, although both have a small bias of approximately 0.03. The OFES and the ECCO2 model, on the other hand, show a large salinity bias of more than 0.10. Such salinity biases in NADW have been found before in numerical models. De Jong et al. [2009] compared several IPCC models and reanalyses and found that most of them are too salty in the Labrador Sea.

The pattern of salinity in the North Atlantic from OFES agrees reasonably well with the climatologies (Fig 11, compare to the same maps for the climatologies in Fig 8). The location and shape of the MOW salt tongue and the Labrador Sea minimum compare well with the HydroBase2 and WOA05 climatologies, although the range of salinity is much smaller, particularly because the MOW is approximately 0.30 too fresh. Nakamura and Kagimoto [2006] reported before that the MOW in OFES is too fresh, due to the very weak outflow of Mediterranean Water into the Gulf of Cádiz. Although the magnitude of the salinity gradient in OFES is too small, the model does show the same linear increase of salinity along the pathway of the DWBC as the two climatologies (Fig 11b), albeit with a much smaller range (0.03 in OFES compared to 0.10 in the climatologies). The OFES model, despite its bias within the Labrador Sea, shares most key features with the observations. All the other models have key shortcomings: DePreSys has almost no decadal variability at the Abaco line, SODA has too large and wrong sign variability, and the ECCO2 run is too short. Hence, the OFES model will be used to study the advective pathways leading to the Abaco line.

3.4. The advection of salinity anomalies in models

The advection of salinity anomalies in the DWBC core along the western Atlantic continental slope can be visualized in a Hovmoller diagram of the OFES model data (left

panels in Fig 12). For these DWBC anomalies, the depth-averaged salinity in the cLSW range was extracted for each grid point 0.3° from the western Atlantic shelf between 50°N and 23°N, the DWBC path also used in Fig 11a. In the Labrador Sea (on the right side of Fig 12a, see also Fig 10b), three major freshening events can be observed after 1970: one in the mid 1970s which coincides with the Great Salinity Anomaly of the 1970s [Dickson et al., 1988], one in the mid 1980s which coincides with the Great Salinity Anomaly of the 1980s [Belkin et al., 1998], and one in the early 1990s which matches the Great Salinity Anomaly of the 1990s [Belkin, 2004].

All three of these major freshening events propagate southward along the continental slope (Fig 12a). The 1970s event does not seem to propagate much farther south than 40°N, while the events in the mid 1980s and in the early 1990s cause downstream freshening all the way to Abaco. In the Labrador Sea the latter two events are separated by a short period of more saline water, but at lower latitudes the two anomalies appear to merge into one and trigger the 1995 freshening at the Abaco line.

While moving southward, the salinity signals get diluted, just as in the hydrographic observations. The standard deviation of salinity along the DWBC core decreases equatorward by more than a factor three (Fig 11a), from 0.025 near the Grand Banks to 0.008 at Abaco (Fig 12c). Most of the decrease in variability (from 0.025 to 0.011) occurs along the northern half of the path, north of 40°N.

The speed of advection can be estimated using lagged correlations between time series at different locations along the DWBC core. The highest correlation between the time series at 47°N and 26°N, a distance of 4800 km, occurs at a lag of 10 to 12 years ($R = 0.77$, see Fig 12e), slightly larger than the 9 years lag estimated from the hydrographic data.

Assuming a direct route, the anomalies thus propagate with an average speed of 1.2–1.5 cm/s from the Labrador Sea to the Abaco line. Such speeds agree with estimates of the advection speed from observations. Curry et al. [1998] found a lag of 6 years for a roughly 3000 km distance, or a typical speed of 1.6 cm/s, between the Labrador Sea and Bermuda. Bower et al. [2009] found that Lagrangian floats that move southwestward from Flemish Cap bridge a typical distance of 1000 km in 2 years, also 1.6 cm/s.

The speed along the DWBC as deduced from Fig 12e is, however, not constant. North of 40°N the lag increases more with distance than south of 40°N, implying slower average transit speeds north of that latitude than south of it. The variation in average advection speed along the DWBC core might be related to detrainment into recirculation gyres such as the Worthington gyre [e.g. Hogg 1983] and Northern Recirculation Gyre [e.g. Pickart and Hogg 1989] and possible 'breakpoints' between these [see also Gary et al. 2011]. Within the recirculation gyres the advection of salinity is relatively fast, while the signal takes considerably more time to cross the gyre fronts. The location of the inter-gyre boundary can vary over time, which might explain why the break-point in Fig 12e is rather noisy.

The propagation of signals along internal pathways as found by Bower et al. [2009] and Gary et al. [2011] can be assessed by computing a Hovmoller diagram of salinity along one such interior paths, roughly 500 km away from the continental shelf (right panels in Fig 12). This path starts somewhat more northward of the Grand Banks than the DWBC path (see also Fig 11a), an area where the standard deviation of salinity is somewhat smaller, at 0.020. Along this interior path, the decrease in lead to the Abaco line is more uniform than along the DWBC (Fig 12f, compare with Fig 12e). Particularly beyond the

2500 km point, south of 40°N in the subtropical gyre, the transit speed appears rather uniform at 3000 km in 5 years, or an average transit speed of 2 cm/s. Somewhat faster transit speeds can be seen in the first 1500 km around the Grand Banks, while propagation in the region between 1500 and 2000 km south of Newfoundland is much slower.

For a more basin-wide picture of the advective pathways to Abaco, one can calculate correlations between the salinity at the Abaco line and all other grid points in the basin, an extension of Figs 12e and 12f for the entire North Atlantic basin. This approach follows the technique used by Van der Werf et al. [2009], who evaluated lagged correlations to track the origin and pathway of a salinity anomaly observed along a mooring section in the Mozambique Channel. The lagged correlation of the cLSW salinity anomaly time series between each grid point in the North Atlantic basin and a base point is computed. Here, we use two base points; one at the Abaco line and one in the Labrador Sea. The correlation value R is then calculated as a function of lag and location in the basin. At each location, the lag where R attains its maximum is defined as the most probable lag. In this way, one obtains values for the maximum correlation, the regression, and its associated most probable lag. A map of the maximum correlation (Fig 13a) reveals that for many locations, especially in the eastern subtropical Atlantic Ocean, the correlations with the Abaco line is low and not significant. We mask those areas where the maximum correlation is lower than 0.75.

The largest correlations to the Abaco base point (Fig 13a) are found in the vicinity of the Abaco line and correlations are higher than 0.90 in most of the subtropical Atlantic to the west of the Mid-Atlantic Ridge. In the Labrador Sea it is slightly lower than 0.8, in relatively good agreement with the correlation between the two observational time series.

Note that the correlation with the Abaco line is actually larger in the Icelandic Basin than in the Labrador Sea. The regression coefficient, which is a measure of relative size of the magnitude of salinity anomalies, is roughly 2 in the Labrador Sea and reaches 3 on the southeastern side of Greenland (Fig 13b). This is in agreement with the factor 2 decrease in the magnitude of the salinity anomaly observed in the hydrography. Most of this decrease occurs north of 40°N, while southwest of the Grand Banks the regression of the time series with the model Abaco time series is almost 1.

We have seen that the advection time scale between the Abaco line and the Labrador Sea estimated along the DWBC is around 12 years (Figs 12e and 12f). Here, we show both the leads computed to Abaco (Fig 14a) and lags computed from the Labrador Sea (Fig 14b), to reveal the pathways of cLSW in the model. Note that, since not all variability at any grid cell can be explained by either the Labrador Sea time series or the Abaco time series, the details of the lag plots do not need to be consistent. Furthermore, since the Labrador Sea time series is averaged over a larger domain, it is smoother and therefore the map of lags in Fig 14b is less patchy than that in Fig 14a.

Both the leads from the Abaco base point (Fig 14a) as well as the lags from the Labrador Sea base point (Fig 14b) show large gradients in time lag just south of Newfoundland, at 50°W. The lags from the Labrador Sea increase from less than 3 years on the eastern side of the Grand Banks to more than 7 years on the western side of the Grand Banks. Furthermore, the correlations with the time series at the Abaco base point (Fig 13a) are relatively low in this region. These large gradients and low correlations again suggest a breakpoint in the advective pathways south of Newfoundland and the Grand Banks, with two rather distinct circulations northeast and southwest of 50°W. It is in this region where

Bower et al. [2009 , 2011] and Gary et al. [2011] showed that the interior path of the NADW breaks up into eddies, when the curvature of the continental shelf expels some of the water out of the DWBC.

In the subtropical Atlantic, southwest of the Grand Banks, the lead and lag maps (Fig 14), together with the map of correlations (Fig 13a), are suggestive of an interior pathway of the NADW. The region of significant correlation in the western subtropical Atlantic is much broader than the typical width of the DWBC (order 100 km). Hence, it appears that signals propagate through an interior pathway in this region, similar to what was found by Bower et al. [2009], Zhang [2010], and Gary et al. [2011] in models and observations.

However, the DWBC itself it also clearly visible on the lead and lag maps by a strong offshore gradient in lead/lag in the DWBC northeast of 35°N. The values of leads and lags close to the continental shelf are different from those in the interior, with leads to the Abaco line a few years larger in the DWBC (and, consistently, smaller lags from the Labrador Sea). These larger leads can be explained by assuming that initially the salinity signal travels through the DWBC, during which it is leaked into the interior before it reaches 35°N, probably by eddy mixing. The eddy circulation in the interior then acts to homogenize the salinity signal, similar to the homogenization of potential vorticity by eddies in that region described by Gary et al. [2011], after which the signal is advected southwestward to the Abaco line. Indeed, the map of mean climatological velocity in the cLSW layer (Fig 1) shows a rather broad band of relatively strong southwestward velocities on the southeastern side of the region of significant correlation.

There are more pathways visible in the lead and lag maps (Fig 14). From both base points in Fig 14, there is a tongue of high correlation in the Iceland basin, into the Iceland-

Scotland Overflow pathway. The time lag moving eastward along this tongue increases, meaning this region lags the Labrador Sea changes. The gradual increase in lag from the Labrador and Irminger Seas towards this tongue suggests a direct path between the two sites. This eastward spreading of cLSW has been noted before [e.g. Talley and McCartney, 1982; Rhein et al., 2002; Yashayaev et al., 2007a; Van Aken et al., 2011]. The fact that in the Icelandic Basin the correlation increases as the lead with the Abaco line decreases, suggests that mixing modifies the signals on both pathways in a similar way.

Corroborating our previous results (section 3.2) where we found that the variability in cLSW at Abaco could be explained by the observed variability in the Labrador Sea without requiring any variability in MOW properties, OFES shows no pathway between the Gulf of Cádiz and Abaco. Although there are patches of high correlations in the Gulf of Cádiz, they are isolated and their lag and lead times do not add up, so they cannot be interpreted as advective pathways. This result is the third piece of evidence presented here (after the lagged correlation in hydrography in section 3.1 and the small amount of MOW needed to explain the increase of salinity along the DWBC in section 3.2) that the variability in water mass properties observed at the Abaco line can directly be traced back to variability in the subpolar North Atlantic Ocean.

4. Conclusions and discussion

We have shown, using more than 25 years of repeated hydrographic observations, that water mass variability of classical Labrador Sea Water (cLSW) as measured on the Abaco line near the Bahamas at 26°N can be related to variability in the Labrador Sea 9 years earlier. Although the magnitude of the variability decreases by a factor of 2 between the Labrador Sea and Abaco, the signal stays relatively coherent in time. Mediterranean

Outflow Water (MOW) increases the salinity in the Atlantic basin in the density range of cLSW, and makes up 20% of the water in that layer at Abaco. However, variability of MOW has a negligible effect on salinity variability in the Deep Western Boundary Current (DWBC) at Abaco. The OFES model, which shares many of the characteristics of the observations, has been used to study how salinity anomalies spread throughout the North Atlantic basin, both forward in time from the Labrador Sea and backwards in time from the Abaco line. The maps of lead and lag times to these two base points suggests that the DWBC carries anomalies southward relatively fast, but that eddy mixing removes any offshore gradients before the signal reaches 35°N.

While the correlation and regression between the salinity time series in the Labrador Sea and at the Abaco line are similar in the model and observations, the 10–12 years lag in the model is slightly longer than the 9 years lag in the observational data. This might be related to a number of reasons, including different circulation patterns, lower Eulerian velocities, or different mixing. However, without many more observations in the North Atlantic it will be hard to pinpoint what really causes the difference. In any case, we feel that the difference in lags between the model and the observational data is small enough for the model to be a valuable extra tool for studying hwat the pathway between the Labrador Sea and the Abaco line looks like.

As an interesting side-result, this study shows that none of the three assimilative models analysed here can accurately reproduce the water mass changes along the two hydrographic sections. This is especially concerning, since their rationale is to represent the state of the ocean as closely as possible. OFES, on the other hand, captures all three documented Great Salinity Anomalies (Fig 12), as well as the sudden freshening at the Abaco

line that initiated this study (Fig 10) and the time lag it takes to advect these anomalies southwards. This study can therefore raise confidence in this type of high-resolution numerical models for studying the circulation in the deep ocean.

Bower et al. [2009] found that much of the water in the DWBC is expelled around the Grand Banks and from there follows a broad path in the basin interior. This would intuitively suggest a wide variety of time scales and therefore that signals of water mass change would be smeared out when reaching the subtropics. However, in this study we find significant variability at Abaco, which we can relate to variability in the high-latitude North Atlantic. This is hard to reconcile with studies of ocean mixing using transit time distributions [e.g. Haine and Hall, 2002; Peacock and Maltrud, 2006], where it is typically found that age distributions at a particular location away from the source region are so broad that the standard deviation in age distribution is of the same order of magnitude as the mean age of the water, smearing out short-variability signals. Here, in contrast, we find that the cLSW signals at the Abaco line are fairly similar in shape to the signals when they formed.

The analytical model of Waugh and Hall [2005], for example, was not able to explain how decadal variability of cLSW formation could be observed as far south as Abaco. The model of Waugh and Hall [2005] is an advective-diffusive model of the DWBC: a narrow boundary current of constant width and constant advection velocity in contact with a motionless interior. Tracers can mix between the two regions, and the speed with which they mix is set by a simple relaxation time scale. Using values they deemed appropriate, Waugh and Hall [2005] found that an anomaly was reduced to typically 2% of its magnitude 5000 km away from the source. However, in this study we find amplitude

decays of 50% and time lags of 10 years. The model of Waugh and Hall [2005] can be inverted, solving for the current advection velocity, current width, and mixing time scale, while using the amplitude decay and time lag as input. Doing so yields solutions only if the mixing time scale is shorter than 4 months. That leads to a time scale of a factor 3 smaller than what those authors themselves obtain from analysis of CFC data. Interestingly, therefore, only the assumption of an extremely leaky DWBC, with relatively short mixing time scales, can explain the large coherence of the signal at Abaco. Indeed, the analysis of basin-wide correlations and lags with respect to the Abaco line (Fig 14) shows a more than 1000 km wide band in the subtropical gyre of cross-current uniform lags and correlations. It might be, therefore, that the DWBC is very leaky indeed.

Acknowledgments

This research was supported by the U.S. National Science Foundation under Award OCE0241438. The work of two authors (MB and CM) on this project was also supported by the NOAA Atlantic Oceanographic and Meteorological Laboratory. The OFES simulation was conducted on the Earth Simulator under the support of JAMSTEC. The Labrador Sea time series was constructed with public data (until 1997) as well as post-WOCE data processed by Dr. Igor Yashayaev from the Bedford Institute of Oceanography.

References

Baringer, M. O., Price, J. F., 1997. Mixing and spreading of the Mediterranean Outflow. J. Phys. Oceanogr. 27, 1654–1677.Beal, L. M., Ffield, A., Gordon, A. L., 2000. Spreading of Red Sea overflow waters in the Indian Ocean. J. Geophys. Res. 105, 8549–8564. Belkin, I. M., 2004. Propagation of the “Great Salinity Anomaly” of the 1990s

around the northern North Atlantic. Geophys. Res. Lett. 31, L08306. Belkin, I. M., Levitus, S., Antonov, J. I., Malmberg, S.-A., 1998. "Great Salinity Anomalies" in the North Atlantic. Prog. Oceanogr. 41, 1–68. Bower, A. S., Lozier, M. S., Gary, S. F., 2011. Export of Labrador Sea Water from the subpolar North Atlantic: A Lagrangian perspective. Deep-Sea Res. II 58, 1798–1818. Bower, A. S., Lozier, M. S., Gary, S. F., Böning, C. W., 2009. Interior pathways of the North Atlantic meridional overturning circulation. Nature 459, 243–248. Boyer, T. P., Antonov, J. I., Garcia, H. E., Johnson, D. R., Locarnini, R. A., Mishonov, A. V., Pitcher, M. T., Baranova, O. K., Smolyar, I. V., 2006. NOAA Altas NESDIS 60. U.S. Government Printing Office, Ch. World Ocean Database 2005. Bryden, H. L., Johns, W. E., Saunders, P. M., 2005. Deep western boundary current east of Abaco: Mean structure and transport. J. Mar. Res. 63, 35–57. Candela, J., 2001. Mediterranean water and global circulation. In: Siedler, G., Church, J., Gould, J. (Eds.), Ocean Circulation and Climate: Observing and Modelling the Global Ocean. Vol. 77. Elsevier Oceanographic Series, pp. 419–429. Carton, J. A., 2008. A reanalysis of ocean climate using Simple Ocean Data Assimilation (SODA). Mon. Wea. Rev. 136, 2999–3017. Carton, J. A., Chepurin, G., Cao, X., 2000. A Simple Ocean Data Assimilation analysis of the global upper ocean 1950-95. part I: Methodology. J. Phys. Oceanogr. 30, 294–309. Cunningham, S. A., Kanzow, T., Rayner, D., Baringer, M. O., Johns, W. E., Marotzke, J., Longworth, H. R., Grant, E. M., Hirschi, J., Beal, L. M., Meinen, C. S., Bryden, H. L., 2007. Temporal variability of the Atlantic meridional overturning circulation at 26°N. Science 317, 935–938. Curry, R. G., 1996. HydroBase: A database of hydrographic stations and tools for climatological analysis. Tech. Rep. WHOI-96-01, Woods Hole Oceanographic Institution Technical Report.

Curry, R. G., Dickson, B., Yashayaev, I., 2003. A change in the freshwater balance of the Atlantic Ocean over the past four decades. Nature 426, 826–829. Curry, R. G., McCartney, M. S., 2001. Ocean gyre circulation changes associated with the North Atlantic Oscillation. J. Phys. Oceanogr. 31, 3374–3400. Curry, R. G., McCartney, M. S., Joyce, T. M., 1998. Oceanic transport of subpolar climate signals to mid-depth subtropical waters. Nature 391, 575–577. De Jong, M. F., Drijfhout, S. S., Hazeleger, W., Van Aken, H. M., Severijns, C. A., 2009. Simulations of hydrographic properties in the Northwestern North Atlantic Ocean in Coupled Climate Models. J. Clim. 22, 1767–1786. Dickson, B., Yashayaev, I., Meincke, J., Turrell, B., Dye, S., Holfort, J., 2002. Rapid freshening of the deep North Atlantic Ocean over the past four decades. Nature 416, 832–837. Dickson, R., Lazier, J., Meincke, J., Rhines, P. B., Swift, J., 1996. Long-term coordinated changes in the convective activity of the North Atlantic. Prog. Oceanogr. 38, 241–295. Dickson, R. R., Brown, J., 1994. The production of North Atlantic deep water: sources, rates, and pathways. J. Geophys. Res. 99, 12319–12341. Dickson, R. R., Meincke, J., Malmberg, S.-A., Lee, A. J., 1988. The "Great Salinity Anomaly" in the northern North Atlantic, 1968–1982. Prog. Oceanogr. 20, 103–151. Fine, R. A., Molinari, R. L., 1988. A continuous deep western boundary current between Abaco (26.5°N) and Barbados (13°N). Deep-Sea Res. 35, 1441–1450. Fischer, J., Visbeck, M., Zantopp, R., Nunes, N., 2010. Interannual to decadal variability of outflow from the Labrador Sea. Geophys. Res. Lett. 37, L24610. Gary, S. F., Lozier, M. S., Böning, C. W., Biastoch, A., 2011. Deciphering the pathways for the deep limb of the Meridional Overturning Circulation. Deep-Sea Res. II 58 1781–1797. Hacker, P., Firing, E., Wilson, W. D., Molinari, R. L., 1996. Direct observations of the current

structure east of the Bahamas. Geophys. Res. Lett. 23, 1127–1130. Haine, T. W. N., Hall, T. M., 2002. A generalized transport theory: Water-mass composition and age. J. Phys. Oceanogr. 32, 1932–1946. Hall, M. M., Joyce, T. M., Pickart, R. S., Smethie Jr., W. M., Torres, D. J., 2004. Zonal circulation across 52°W in the North Atlantic. J. Geophys. Res. 109, C11008. Henry-Edwards, A., Tomczak, M., 2006. Detecting changes in Labrador Sea Water through a water mass analysis of BATS data. Ocean Sci. 2, 19–25. Hogg, N. G., 1983. A note on the deep circulation of the western North Atlantic: its nature and causes. Deep-Sea Res. 30, 945–961. Iorga, M. C., Lozier, M. S., 1999. Signatures of the Mediterranean outflow from a North Atlantic climatology 1. salinity and density fields. J. Geophys. Res. 104, 25985–26009. Johns, W. E., Kanzow, T., Zantopp, R., 2005. Estimating ocean transports with dynamic height moorings: An application in the Atlantic Deep Western Boundary Current at 26°N. Deep-Sea Res. I 52, 1542–1567. Joyce, T. M., Dunworth-Baker, J., Pickart, R. S., Torres, D. J., Waterman, S., 2005. On the Deep Western Boundary Current south of Cape Cod. Deep-Sea Res. II 52, 615–625. Kieke, D., Rhein, M., Stramma, L., Smethie Jr., W. M., LeBel, D. A., Zenk, W., 2006. Changes in the CFC inventories and formation rates of Upper Labrador Sea Water, 1997–2001. J. Phys. Oceanogr. 36, 64–86. Leadbetter, S. J., Williams, R. G., McDonagh, E. L., King, B. A., 2007. A twenty year reversal in water mass trends in the subtropical North Atlantic. Geophys. Res. Lett. 34, L12608. Lee, T. N., Johns, W. E., Schott, F. A., Zantopp, R. J., 1990. Western boundary current structure and variability east of Abaco, Bahamas at 26.5°N. J. Phys. Oceanogr. 20, 446–466. Lee, T. N., Johns, W. E., Zantopp, R. J., Fillenbaum, E. R., 1996. Moored observations of western boundary current variability and thermohaline circulation at 26.5°N in the

subtropical North Atlantic. J. Phys. Oceanogr. 26, 962–983. Marshall, J., Adcroft, A., Hill, C., Perelman, L., Heisey, C., 1997. A finite-volume, incompressible Navier Stokes model for studies of the ocean on parallel computers. J. Geophys. Res. 102, 5753–5766. McCartney, M. S., 1992. Recirculating components to the deep boundary current of the northern North Atlantic. Prog. Oceanogr. 29, 283–383. McDougall, T. J., Jackett, D. R., 2005. The material derivative of neutral density. J. Mar. Res. 63, 159–185. Meinen, C. S., Baringer, M. O., Garzoli, S. L., 2006. Variability in Deep Western Boundary Current transports: Preliminary results from 26.5°N in the Atlantic. Geophys. Res. Lett. 33, L17610. Meinen, C. S., Garzoli, S. L., Johns, W. E., Baringer, M. O., 2004. Transport variability of the Deep Western Boundary Current and the Antilles Current off Abaco Island, Bahamas. Deep-Sea Res. I 51, 1397–1415. Menemenlis, D., Fukumori, I., Lee, T., 2005. Using Green's functions to calibrate an ocean general circulation model. Mon. Wea. Rev. 133, 1224–1240. Molinari, R. L., Fine, R. A., Johns, E., 1992. The Deep Western Boundary Current in the tropical North Atlantic Ocean. Deep-Sea Res. 39, 1967–1984. Molinari, R. L., Fine, R. A., Wilson, W. D., Curry, R. G., Abell, J., McCartney, M. S., 1998. The arrival of recently formed Labrador Sea Water in the Deep Western Boundary Current at 26.5°N. Geophys. Res. Lett. 25, 2249–2252. Nakamura, M., Kagimoto, T., 2006. Potential vorticity and eddy potential enstrophy in the North Atlantic Ocean simulated by a global eddy-resolving model. Dyn. Atmos. Oceans 41, 28–59. Paillet, J., Arhan, M., McCartney, M. S., 1998. Spreading of Labrador Sea Water in the eastern North Atlantic. J. Geophys. Res. 103, 10223–10239. Peacock, S., Maltrud, M. E., 2006. Transit-time distributions in a global ocean model. J. Phys. Oceanogr. 36, 474–495. Pickart, R. S., 1992. Water mass components of the

North Atlantic deep western boundary current. Deep-Sea Res. 39, 1553–1572. Pickart, R. S., Hogg, N. G., 1989. A tracer study of the deep Gulf Stream cyclonic recirculation. Deep-Sea Res. 36, 935–956. Potter, R. A., Lozier, M. S., 2004. On the warming and salinification of the Mediterranean outflow waters in the North Atlantic. Geophys. Res. Lett. 31, L01202. Rhein, M., Fischer, J., Smethie Jr., W. M., D., S.-W., Weiss, R. F., Mertens, C., Min, D.-H., Fleischmann, U., Putzka, A., 2002. Labrador Sea Water: Pathways, CFC inventory, and formation rates. J. Phys. Oceanogr. 32, 648–665. Roether, W., Manca, B. B., Klein, B., Bregant, D., Georgopoulos, D., Beitzel, V., Kovačević, V., Luchetta, A., 1996. Recent changes in the Eastern Mediterranean Deep Waters. Science 271, 333–335. Sarafanov, A., Falina, A., Mercier, H., Lherminier, P., Sokov, A., 2009. Recent changes in the Greenland–Scotland overflow-derived water transport inferred from hydrographic observations in the southern Irminger sea. Geophys. Res. Lett. 36, L13606. Sasaki, H., Nonaka, M., Masumoto, Y., Sasai, Y., Uehara, H., Sakuma, H., 2008. High Resolution Numerical Modelling of the Atmosphere and Ocean. Springer New York, Ch. An Eddy-Resolving Hindcast Simulation of the Quasiglobal Ocean from 1950 to 2003 on the Earth Simulator, pp. 157–185. Smith, D. M., Murphy, J. M., 2007. An objective ocean temperature and salinity analysis using covariances from a global climate model. J. Geophys. Res. 112, C02022. Talley, L. D., McCartney, M. S., 1982. Distribution and circulation of Labrador Sea Water. J. Phys. Oceanogr. 12, 1189–1205. Van Aken, H. M., De Jong, M. F., Yashayaev, I., 2011. Decadal and multi-decadal variability of Labrador Sea Water in the northern North Atlantic Ocean derived from tracer distributions: heat budget, ventilation, and advection. Deep-Sea Res. I 58, 505–523. Van der Werf, P. M., Schouten, M. W., Van Leeuwen, P. J., Ridderinkhof, H.,

De Ruijter, W. P. M., 2009. Observation and origin of an interannual salinity anomaly in the Mozambique Channel. J. Geophys. Res. 114, C03017. Vaughan, S. L., Molinari, R. L., 1997. Temperature and salinity variability in the Deep Western Boundary Current. J. Phys. Oceanogr. 27, 749–761. Waugh, D. W., Hall, T. M., 2005. Propagation of tracer signals in boundary currents. J. Phys. Oceanogr. 35, 1538–1552. Worthington, L. V., 1976. On the North Atlantic circualtion. Vol. 6 of Oceanographic Studies. Johns Hopkins University Press. Yashayaev, I., 2007. Hydrographic changes in the Labrador Sea, 1960–2005. Prog. Oceanogr. 73, 242–276. Yashayaev, I., Bersch, M., Van Aken, H. M., 2007a. Spreading of the Labrador Sea Water to the Irminger and Iceland basins. Geophys. Res. Lett. (L10602). Yashayaev, I., Van Aken, H. M., Holliday, N. P., Bersch, M., 2007b. Transformation of the Labrador Sea Water in the subpolar North Atlantic. Geophys. Res. Lett. 34, L22605. Zhang, R., 2010. Latitudinal dependence of atlantic meridional overturning circulation (AMOC) variations. Geophys. Res. Lett. 37, L16703.

Figure 1. Map of the North Atlantic Ocean, depicting the regions of interest for this study (the Abaco line, the Labrador Sea and the Mediterranean Outflow Water region) on top of the climatological velocity field in the OFES model climatology, depth-averaged between the $\sigma_2 = 36.82$ kg/m^3 and $\sigma_2 = 36.97$ kg/m^3 isopycnal surfaces. Velocities in this layer are typically 4 cm/s in the Deep Western Boundary Current. At 5000 km, this implies a lag between the Labrador Sea and Abaco line of approximately 4 years. Molinari et al. [1998], however, found a lag of 10 years; a timescale which is confirmed in this study.

Figure 2. Hovmoller plots of (a) salinity and (b) temperature on the $\sigma_{1.5} = 34.67$ kg/m^3 density surface (the core of the classical Labrador Seawater) just off the Abaco coast. The black plusses indicate locations and timing of CTD stations. Additional CTD stations outside of the domain shown here were used for the interpolation toward the domain boundaries. This figure is an extension of a similar figure (on approximately the same color scale) by Molinari et al. [1998] which showed that between 1994 and 1996 the core of the cLSW freshened and became colder. This extension shows that since then temperature and salinity have not come back to 1980s levels.

Figure 3. The mean profile of neutral density (γ_n), σ_θ, and σ_2 in the DWBC off Abaco (upper panels) and in the Labrador Sea (lower panels). Fine and Molinari [1988] and Molinari et al. [1998] proposed a division in water mass classes based on the hydrography at the Abaco line itself using depth levels (vertical axes in the upper panels). In the Labrador Sea, each of the different density coordinates has a different classification (horizontal axes), proposed by different authors. Part of the differences between the depths of the water masses at the Abaco line can be related to differences in the depths of the water masses in the Labrador Sea itself (lower panels). The classification that best relates the water masses in the Labrador Sea with those at Abaco is that based on σ_2 isopycnals (panels c and f).

Figure 4. Hovmoller plot of the salinity anomaly obtained by averaging the salinity in the first 100 km offshore along σ_2 isopycnals in the DWBC at the Abaco line, with the water mass classification in dashed lines. The black triangles on the top indicate when the sections were occupied. It appears that on decadal timescales cLSW and the two types of overflow water become fresher, while uLSW becomes saltier.

Figure 5. Temperature-salinity diagram of the water mass properties at the Abaco line (thick lines), with one line for each hydrographic section based on averaging water properties along σ_2 surfaces within 100 km of the continental shelf. The thin lines depict the water mass properties in the Labrador Sea, with a 9 year lead. The black lines are the σ_2 isopycnals that delineate the four different water masses. The freshening of the cLSW at Abaco in 1994–1996 is visible, as well as the increase in salinity of the uLSW at that time. The same freshening of cLSW can be seen in the Labrador Sea, with a much larger spread in salinity.

Figure 6. The evolution of salinity anomalies in the cLSW density class (between the $\sigma_2 =$ 36.82 kg/m^3 and $\sigma_2 = 36.97$ kg/m^3 isopycnals) at the Abaco line and in the Labrador Sea. The latter data set was compiled by Van Aken et al. [2011]. The decrease in salinity in the Labrador Sea between 1984 and 1995 leads to a decrease in salinity at the Abaco line starting in 1995. Although not statistically significant, there is a 0.80 correlation at a 9 year lag between the Labrador Sea and the Abaco line, with the amplitude of decadal variability decreased by a factor 2.

Figure 7. Evolution of layer thickness for the four different water masses at the Abaco line. Unlike in the Labrador Sea, where the thickness of uLSW and cLSW vary by more than 1000 m on decadal timescales [Kieke et al., 2006], there is little variability in the thickness of the Labrador Seawater masses at the Abaco line.

Figure 8. Map of cLSW salinity, computed by depth-averaging the salinity between the $\sigma_2 = 36.82$ kg/m^3 and $\sigma_2 = 36.97$ kg/m^3 isopycnal surfaces in (a) the World Ocean Atlas 2005 and (c) the HydroBase2 climatology. The amount of small-scale variability is different between the two climatologies, but the large-scale patterns are similar. Note that the color scale is cut off at 35.14, the core of the MOW is saltier than that at 35.30. The salinity along the western Atlantic continental shelf ((b) and (d), calculated along the black lines in (a) and (c)) shows that for both climatologies the salinity increases approximately linear between 45°N and 25°N.

Figure 9. The mixing fractions of Labrador Seawater and Mediterranean Outflow Water at the Abaco line from the HydroBase2 climatology. (a) Temperature-Salinity diagrams for the HydroBase2 profiles in the Labrador Sea (blue), the Gulf of Cádiz (red), and at the Abaco line (black). See Fig 1for the locations where these profiles are computed. The colored lines denote mean profiles, the shaded areas standard deviations around the means (calculated on σ_2 levels). There is no shading for Abaco since the region is one single grid point. The gray lines are the σ_2 isopycnals that delineate the different water masses. (b) The percentage of Mediterranean Water needed to explain the Abaco profile as a function of σ_2, under the assumption that the rest of the water is Labrador Seawater. The gray area is the 1σ confidence interval. For cLSW, the fraction of Mediterranean Water at Abaco in slightly more than 20%.

Figure 10. Comparison of salinity of the four different numerical models with the hydrography for (a) the Abaco line and (b) the Labrador Sea, computed by depth-averaging the salinity between the $\sigma_2 = 36.82$ kg/m^3 and $\sigma_2 = 36.97$ kg/m^3 isopycnal surfaces. At the Abaco line, OFES follows the hydrography best, with the variability in SODA too large and the decrease in salinity after the 1990s not captured by DePreSys and ECCO2. In the Labrador Sea, SODA and DePreSys follow the hydrography much better. ECCO2 and OFES have a similar decadal variability, but suffer from a bias.

Figure 11. (a) Map of cLSW salinity in the OFES model, computed by depth-averaging the salinity between the $\sigma_2 = 36.82$ kg/m^3 and $\sigma_2 = 36.97$ kg/m^3 isopycnal surfaces, on the same color scale as the map of cLSW salinity in the climatologies (Fig 8). The range of salinity is much smaller in OFES than in the climatologies, but the shape of the MOW tongue and the Labrador Sea minimum is similar. (b) The salinity along the western continental shelf (blue line in (a)) increases approximately linearly from 45°N to 25°N in the OFES model, also similar to what was found in the two climatologies (Fig 8). One difference between the climatologies and OFES, however, is a local maximum in salinity between the Grand Banks and the northern Labrador Sea. This maximum is also responsible for the local minimum in salinity at the 300 km point in panel b.

Figure 12. The advection of salinity anomalies along the DWBC (left panels) and in the interior pathway (righ panels), defined as the blue and red in line in Fig 11b, respectively. (a and b) Hovmoller diagram of salinity from the Labrador Sea (right side) to the Abaco line (left side) in the OFES model. (c and d) The standard deviation in salinity at each grid point for the two pathways. Most of the variability in salinity is damped before the signal reaches 40°N. The decrease in variability is a factor 2 to 3. (e and f) The lead, in years, at which the time series of salinity at each point along the continental shelf has the largest correlation with the time series of salinity at 26°N. The lead increases moving northeastward.

Figure 13. Maps of (a) lagged correlation and (b) regression in the OFES model between the time series of salinity at the Abaco base point (the black circles) and the time series salinity at any other point in the North Atlantic in the cLSW density range. Areas where the correlation is lower than 0.75 are shaded light gray and areas where no correlations have been computed are shaded dark gray. In the model, the correlation between the Labrador Sea and the Abaco line is around 0.8 and the regression is approximately 2. This agrees with the results from the hydrographic time series (Fig 6).

Figure 14. Advection timescales in the OFES model to (a) the Abaco line and from (b) the Labrador Sea, determined from the lag at which correlation is highest between the time series of salinity at the base point (the black circles) and the time series of salinity at any other point in the North Atlantic in the cLSW density range. Areas where the correlation is lower than 0.75 are shaded light gray and areas where no correlations have been computed are shaded dark gray. In the model, the lag between the Labrador Sea and the Abaco line is 10–12 years.

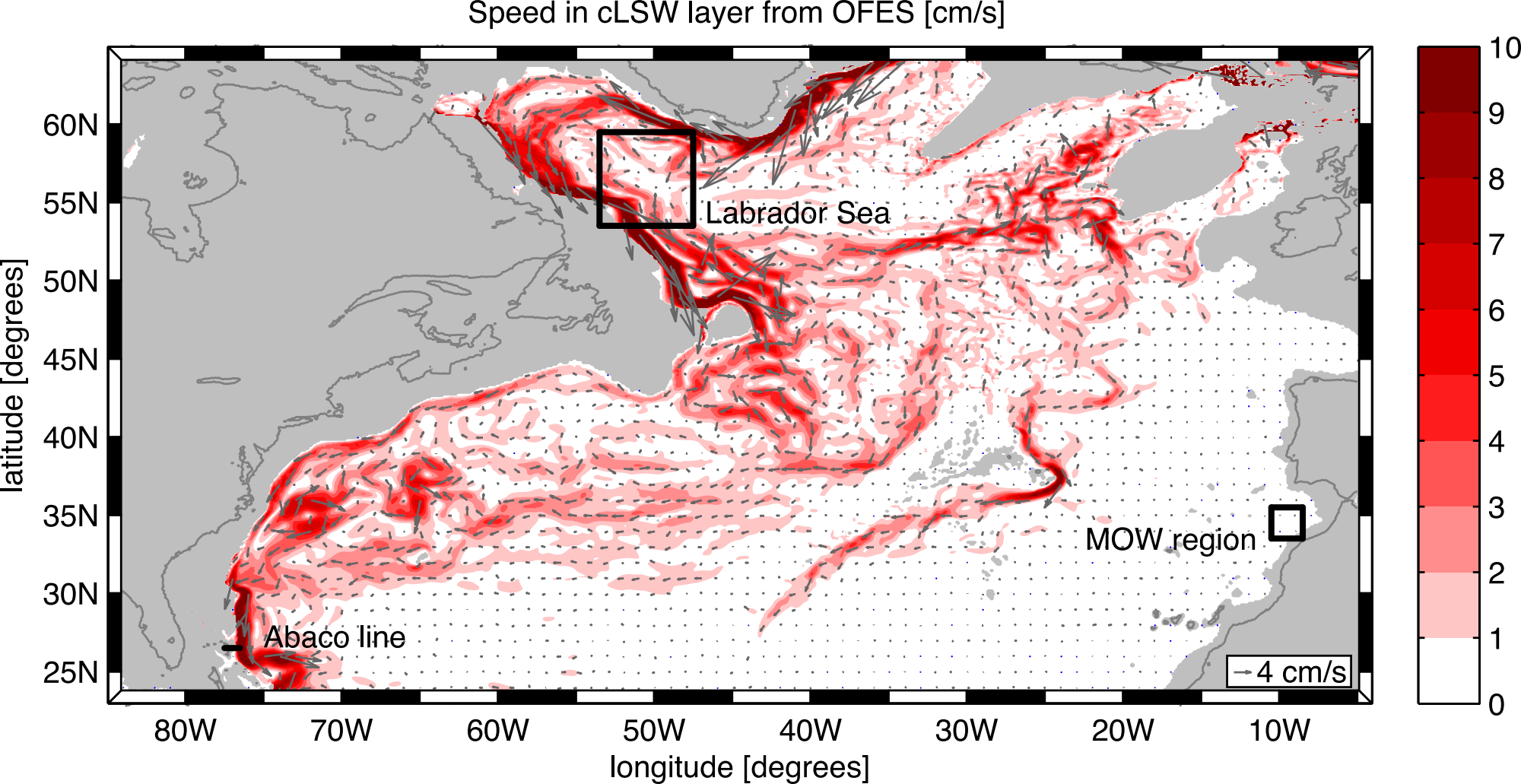
Speed in cLSW layer from OFES [cm/s]
Labrador Sea
MOW region
Abaco line
4 cm/s
60N
55N
50N
45N
40N
35N
30N
25N
latitude [degrees]
80W
70W
60W
50W
40W
30W
20W
10W
longitude [degrees]
10
9
8
7
6
5
4
3
2
1
0

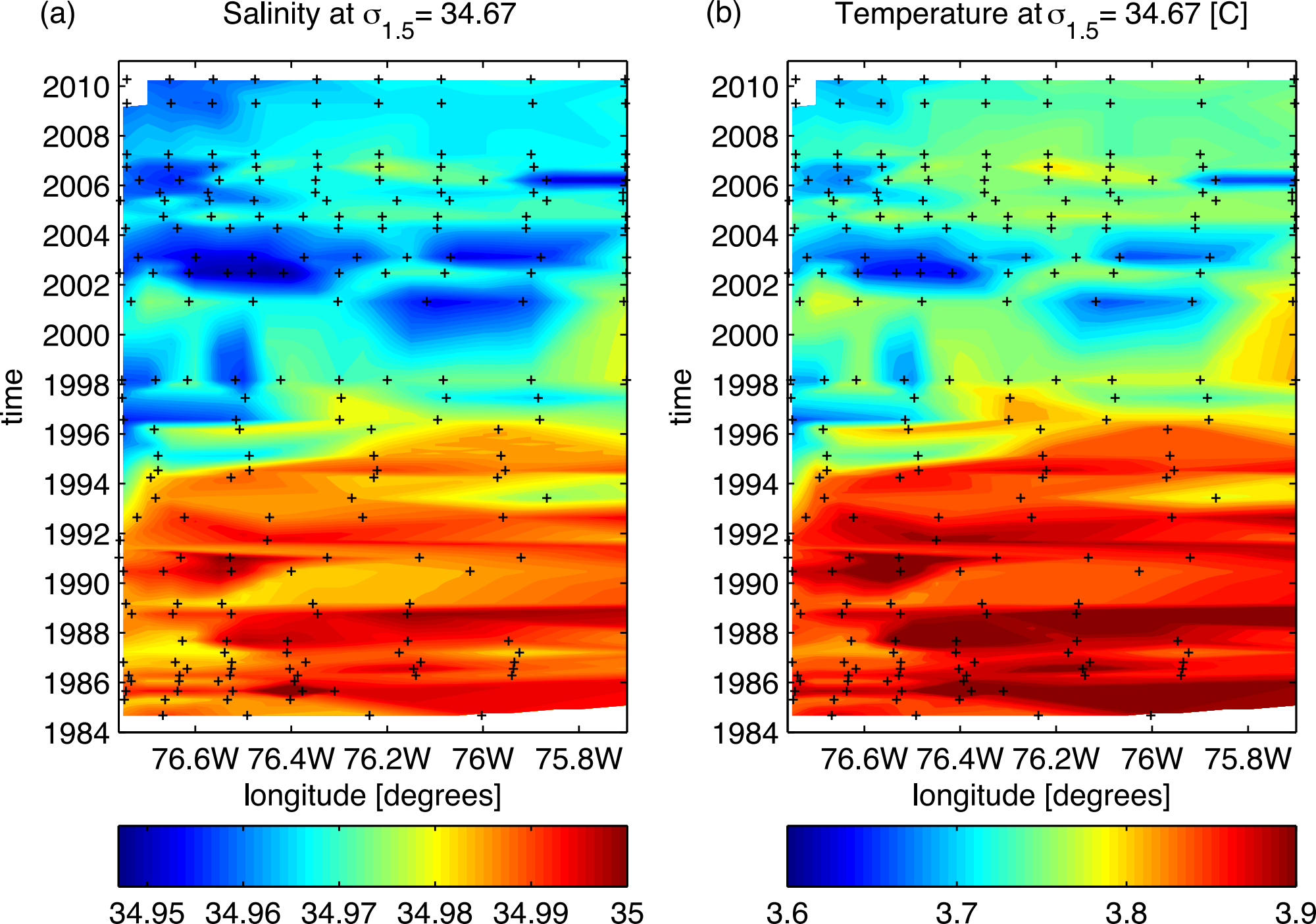
(a)
Salinity at $\sigma_{1.5}$= 34.67
(b)
Temperature at $\sigma_{1.5}$= 34.67 [C]
time
2010
2008
2006
2004
2002
2000
1998
1996
1994
1992
1990
1988
1986
1984
76.6W 76.4W 76.2W 76W 75.8W
longitude [degrees]
34.95 34.96 34.97 34.98 34.99 35
3.6 3.7 3.8 3.9

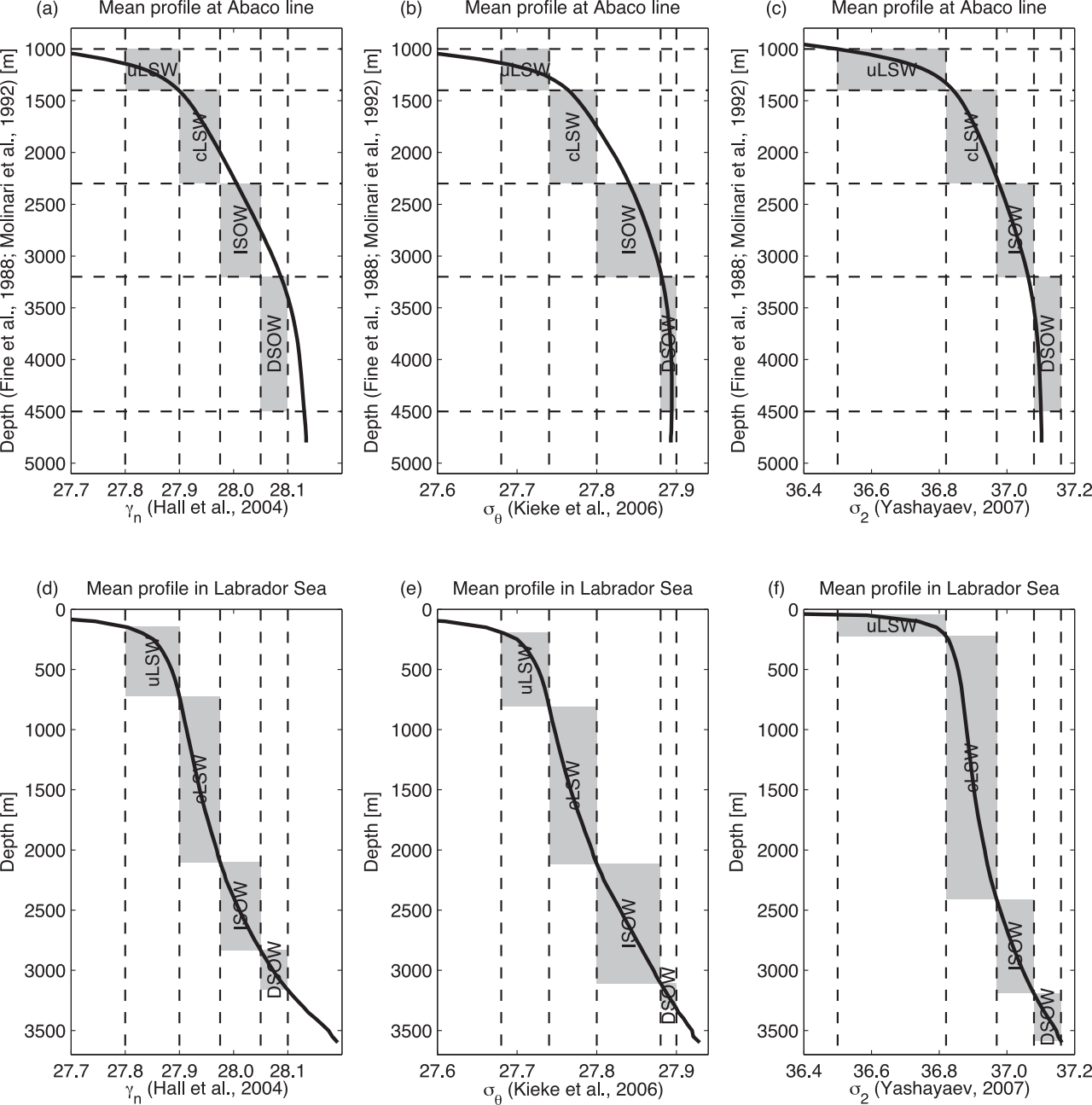
(a)
Mean profile at Abaco line
uLSW
cLSW
ISOW
DSOW
Depth (Fine et al., 1988; Molinari et al., 1992) [m]
1000
1500
2000
2500
3000
3500
4000
4500
5000
27.7
27.8
27.9
28.0
28.1
γn (Hall et al., 2004)
(b)
Mean profile at Abaco line
uLSW
cLSW
ISOW
DSOW
Depth (Fine et al., 1988; Molinari et al., 1992) [m]
27.6
27.7
27.8
27.9
σθ (Kieke et al., 2006)
(c)
Mean profile at Abaco line
uLSW
cLSW
ISOW
DSOW
Depth (Fine et al., 1988; Molinari et al., 1992) [m]
36.4
36.6
36.8
37.0
37.2
σ2 (Yashayaev, 2007)
(d)
Mean profile in Labrador Sea
uLSW
cLSW
ISOW
DSOW
Depth [m]
0
500
1000
1500
2000
2500
3000
3500
27.7
27.8
27.9
28.0
28.1
γn (Hall et al., 2004)
(e)
Mean profile in Labrador Sea
uLSW
cLSW
ISOW
DSOW
Depth [m]
27.6
27.7
27.8
27.9
σθ (Kieke et al., 2006)
(f)
Mean profile in Labrador Sea
uLSW
cLSW
ISOW
DSOW
Depth [m]
36.4
36.6
36.8
37.0
37.2
σ2 (Yashayaev, 2007)

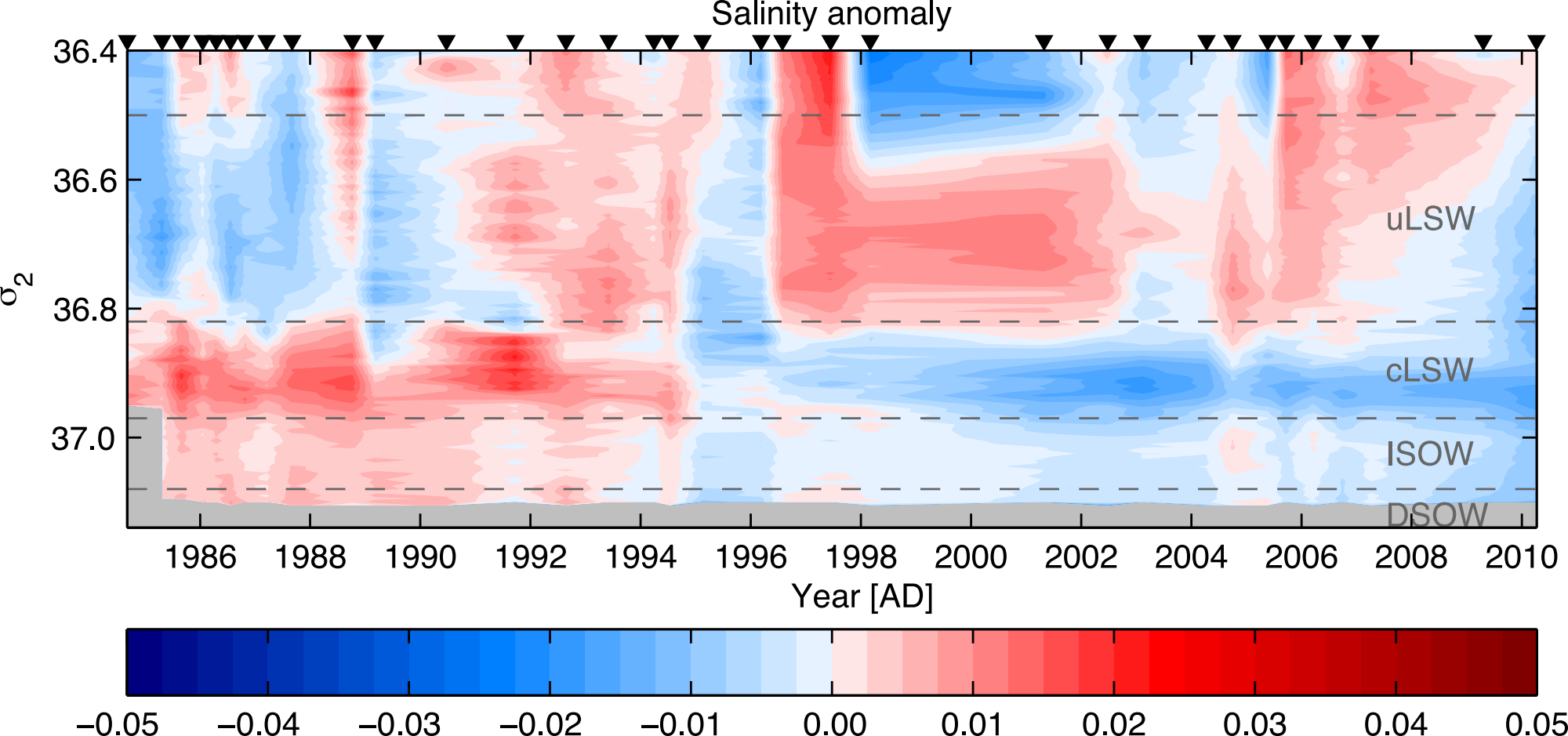
Salinity anomaly
36.4
36.6
36.8
37.0
σ2
uLSW
cLSW
lSOW
DSOW
1986
1988
1990
1992
1994
1996
1998
2000
2002
2004
2006
2008
2010
Year [AD]
−0.05
−0.04
−0.03
−0.02
−0.01
0.00
0.01
0.02
0.03
0.04
0.05

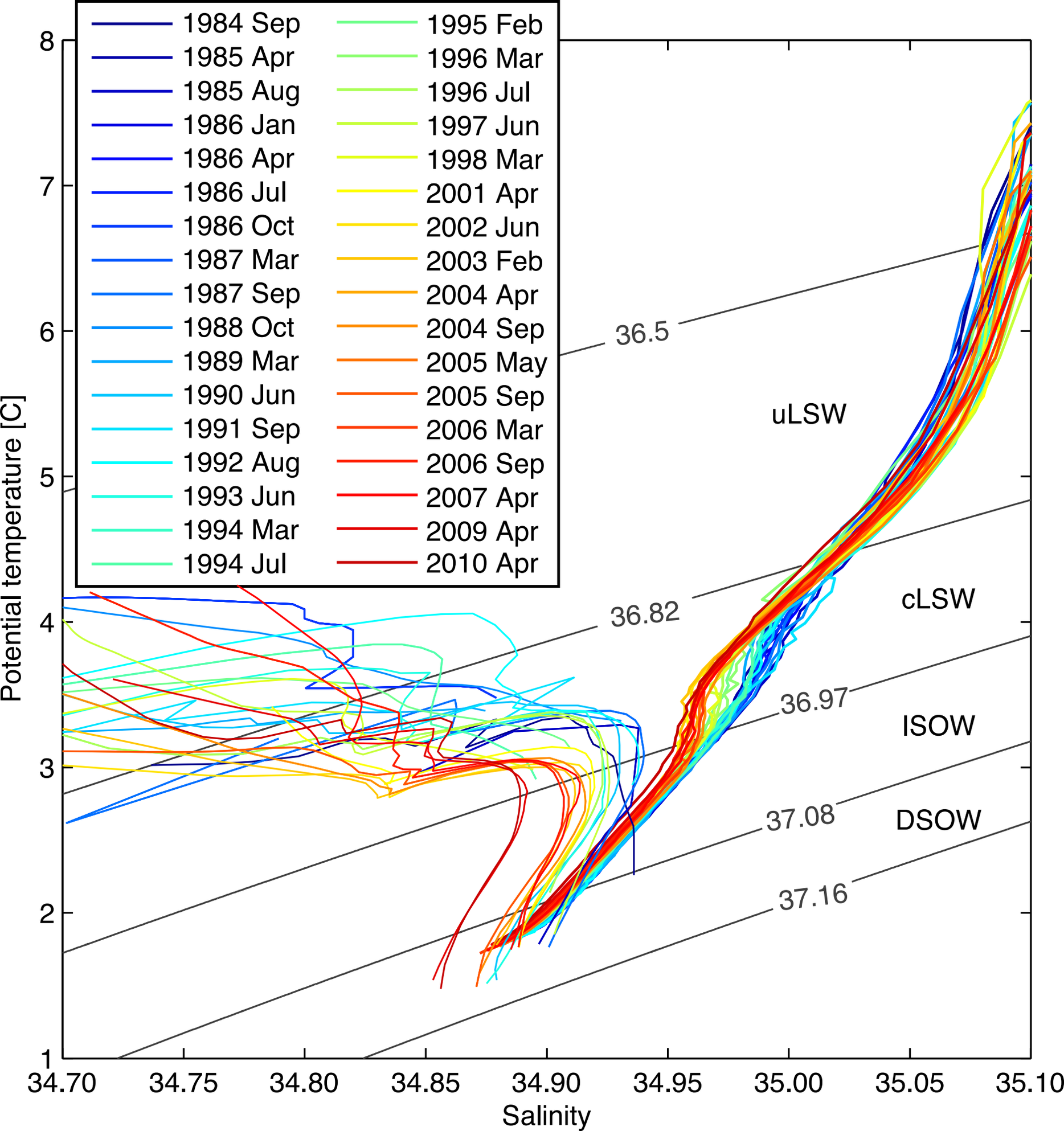
1984 Sep
1985 Apr
1985 Aug
1986 Jan
1986 Apr
1986 Jul
1986 Oct
1987 Mar
1987 Sep
1988 Oct
1989 Mar
1990 Jun
1991 Sep
1992 Aug
1993 Jun
1994 Mar
1994 Jul
1995 Feb
1996 Mar
1996 Jul
1997 Jun
1998 Mar
2001 Apr
2002 Jun
2003 Feb
2004 Apr
2004 Sep
2005 May
2005 Sep
2006 Mar
2006 Sep
2007 Apr
2009 Apr
2010 Apr
36.5
36.82
36.97
37.08
37.16
uLSW
cLSW
ISOW
DSOW
Potential temperature [C]
Salinity
8
7
6
5
4
3
2
1
34.70
34.75
34.80
34.85
34.90
34.95
35.00
35.05
35.10

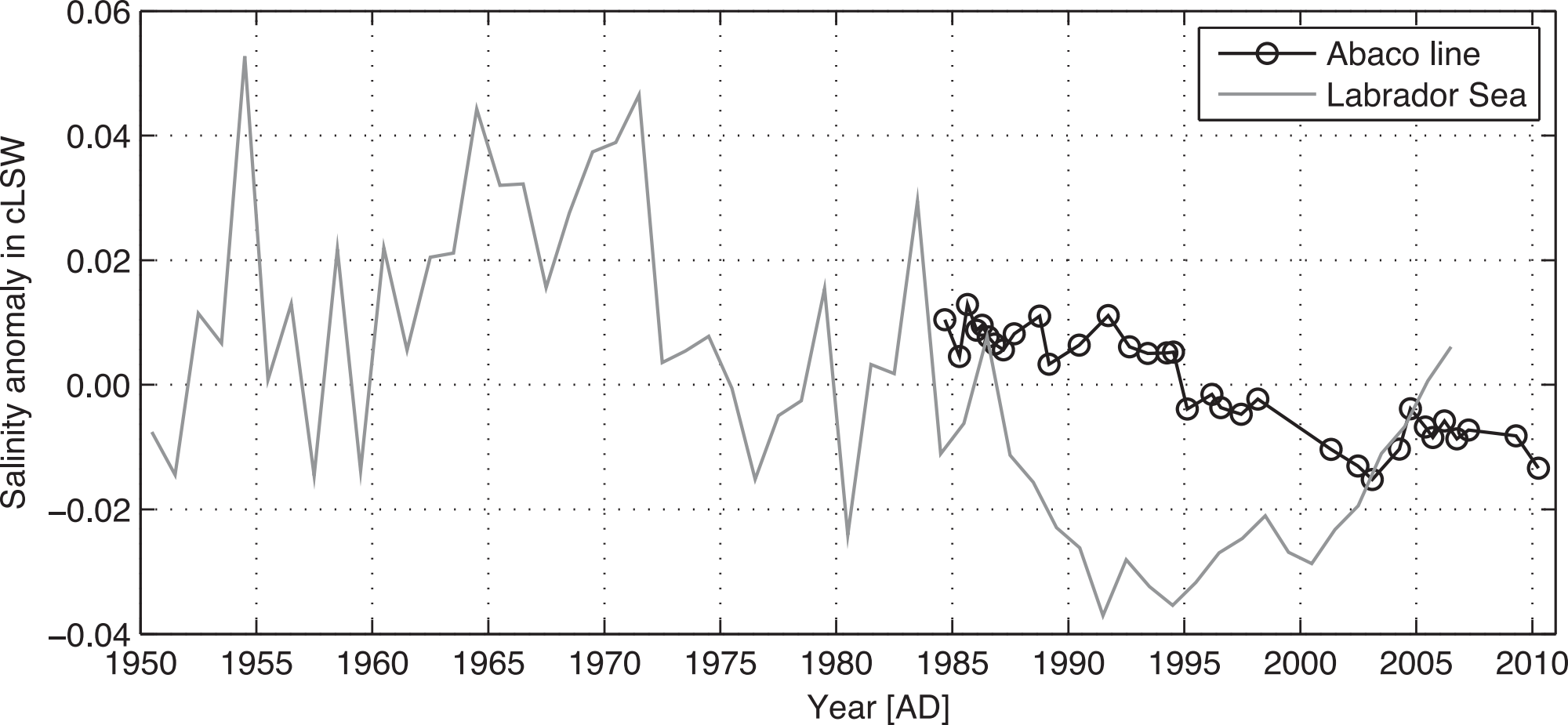
Abaco line
Labrador Sea
Salinity anomaly in cLSW
Year [AD]
0.06
0.04
0.02
0.00
−0.02
−0.04
1950
1955
1960
1965
1970
1975
1980
1985
1990
1995
2000
2005
2010

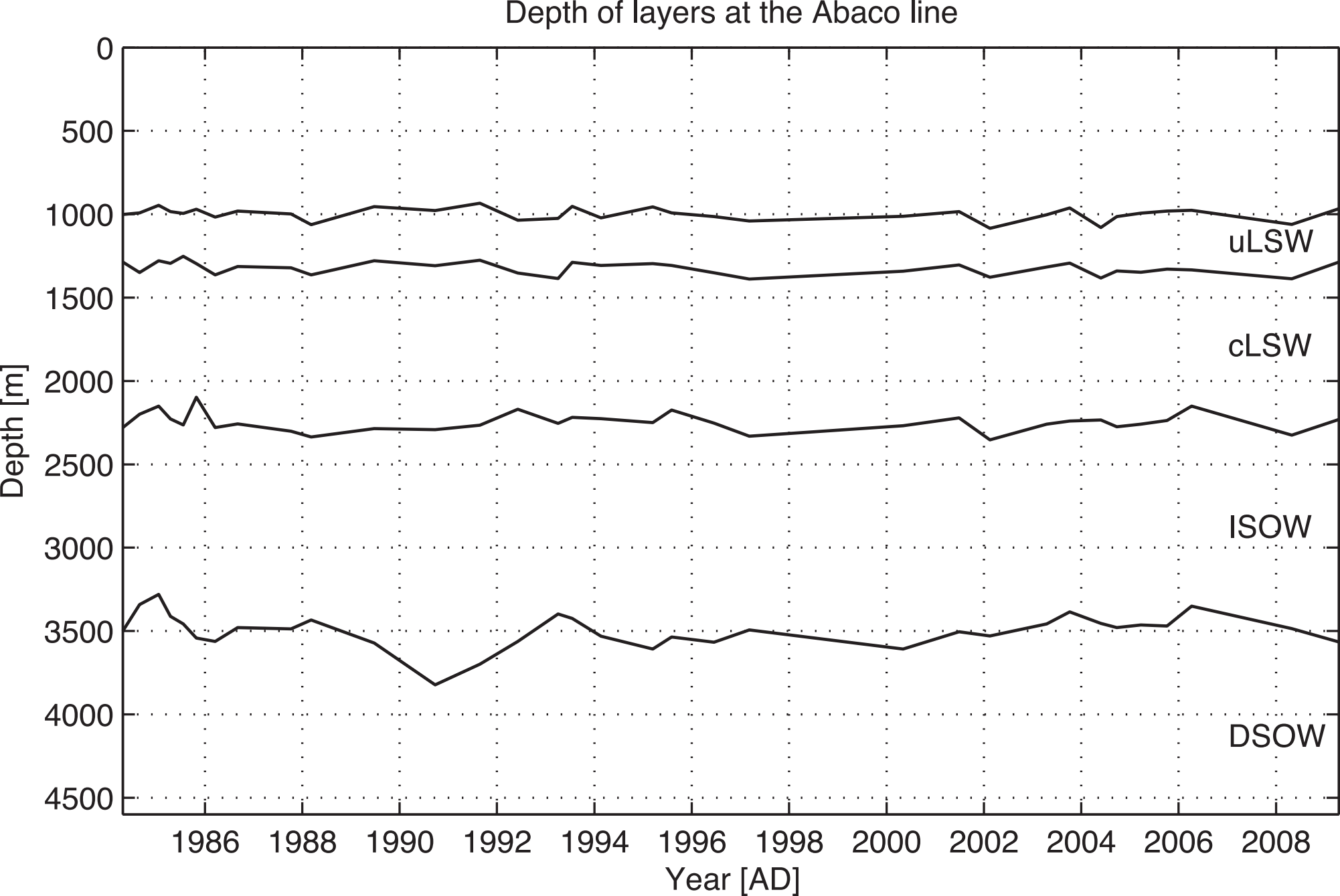
Depth of layers at the Abaco line
0
500
1000
1500
2000
2500
3000
3500
4000
4500
Depth [m]
uLSW
cLSW
ISOW
DSOW
1986
1988
1990
1992
1994
1996
1998
2000
2002
2004
2006
2008
Year [AD]

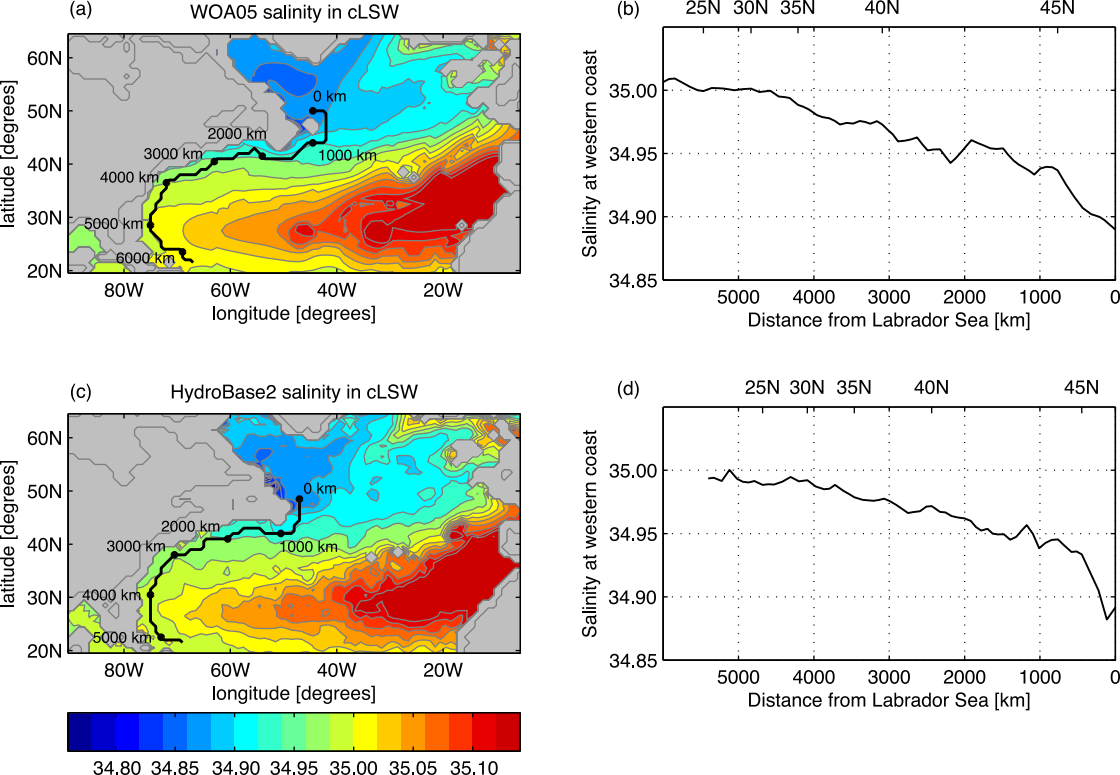
(a)
WOA05 salinity in cLSW
60N
50N
40N
30N
20N
latitude [degrees]
80W
60W
40W
20W
longitude [degrees]
0 km
1000 km
2000 km
3000 km
4000 km
5000 km
6000 km
(b)
25N
30N
35N
40N
45N
Salinity at western coast
35.00
34.95
34.90
34.85
5000
4000
3000
2000
1000
0
Distance from Labrador Sea [km]
(c)
HydroBase2 salinity in cLSW
60N
50N
40N
30N
20N
latitude [degrees]
80W
60W
40W
20W
longitude [degrees]
0 km
1000 km
2000 km
3000 km
4000 km
5000 km
34.80
34.85
34.90
34.95
35.00
35.05
35.10
(d)
25N
30N
35N
40N
45N
Salinity at western coast
35.00
34.95
34.90
34.85
5000
4000
3000
2000
1000
0
Distance from Labrador Sea [km]

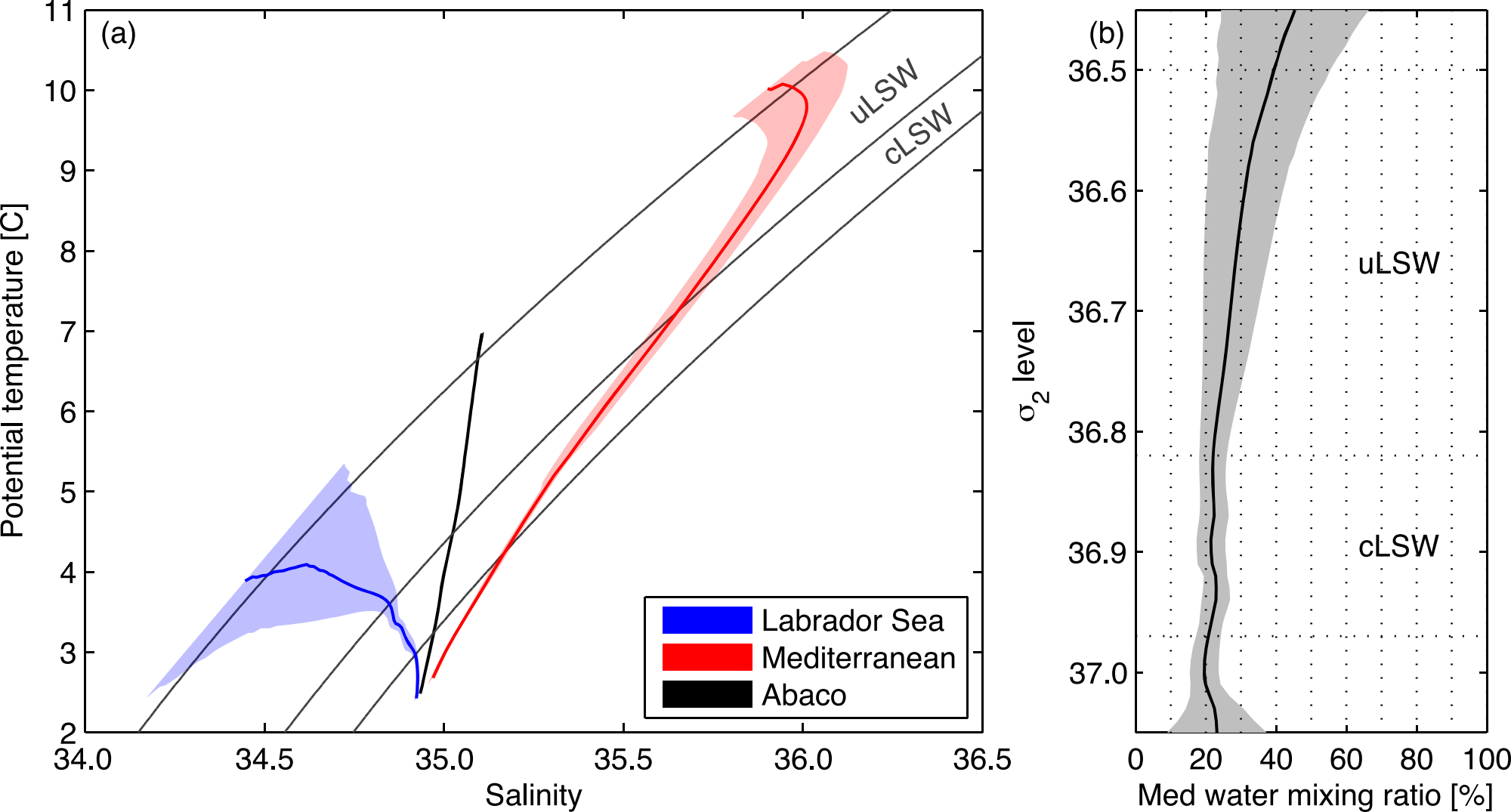
(a)
Potential temperature [C]
Salinity
uLSW
cLSW
Labrador Sea
Mediterranean
Abaco
(b)
σ2 level
Med water mixing ratio [%]
uLSW
cLSW

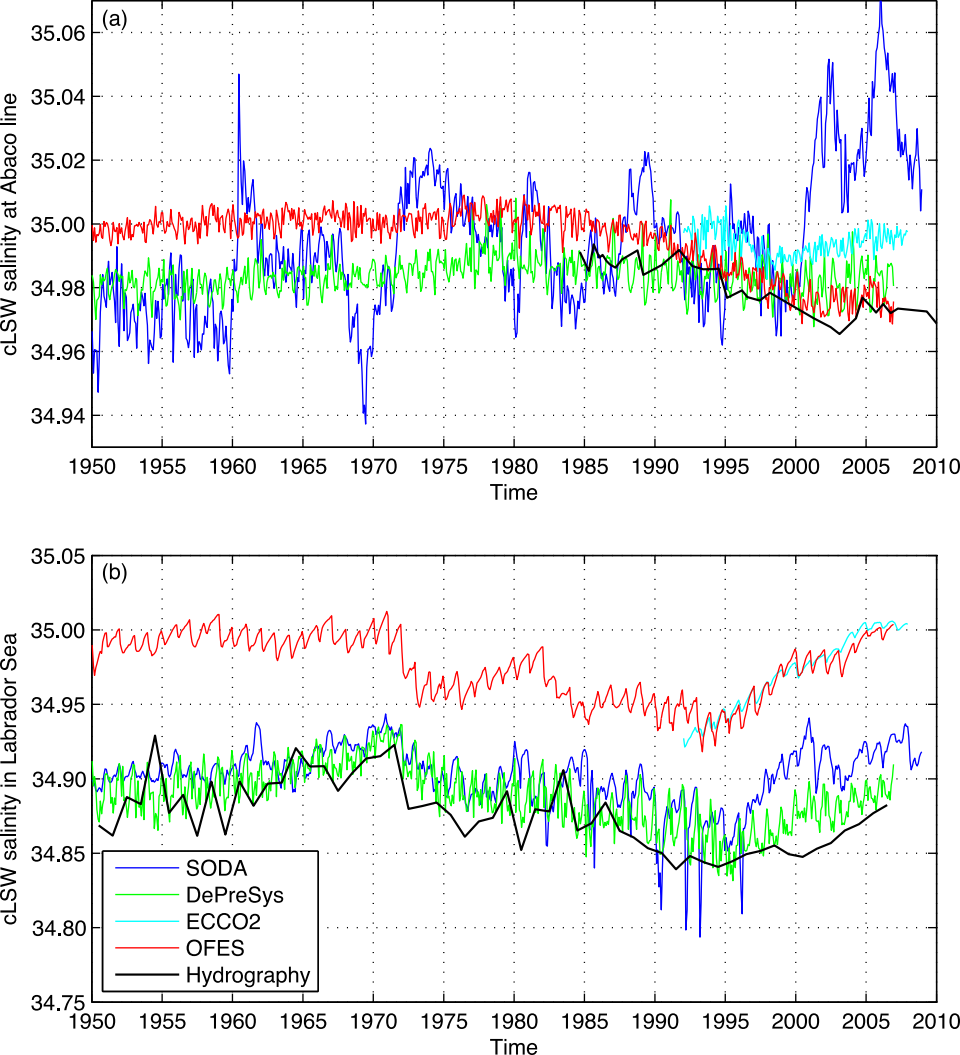
(a)
cLSW salinity at Abaco line
35.06
35.04
35.02
35.00
34.98
34.96
34.94
1950
1955
1960
1965
1970
1975
1980
1985
1990
1995
2000
2005
2010
Time
(b)
cLSW salinity in Labrador Sea
35.05
35.00
34.95
34.90
34.85
34.80
34.75
SODA
DePreSys
ECCO2
OFES
Hydrography
1950
1955
1960
1965
1970
1975
1980
1985
1990
1995
2000
2005
2010
Time

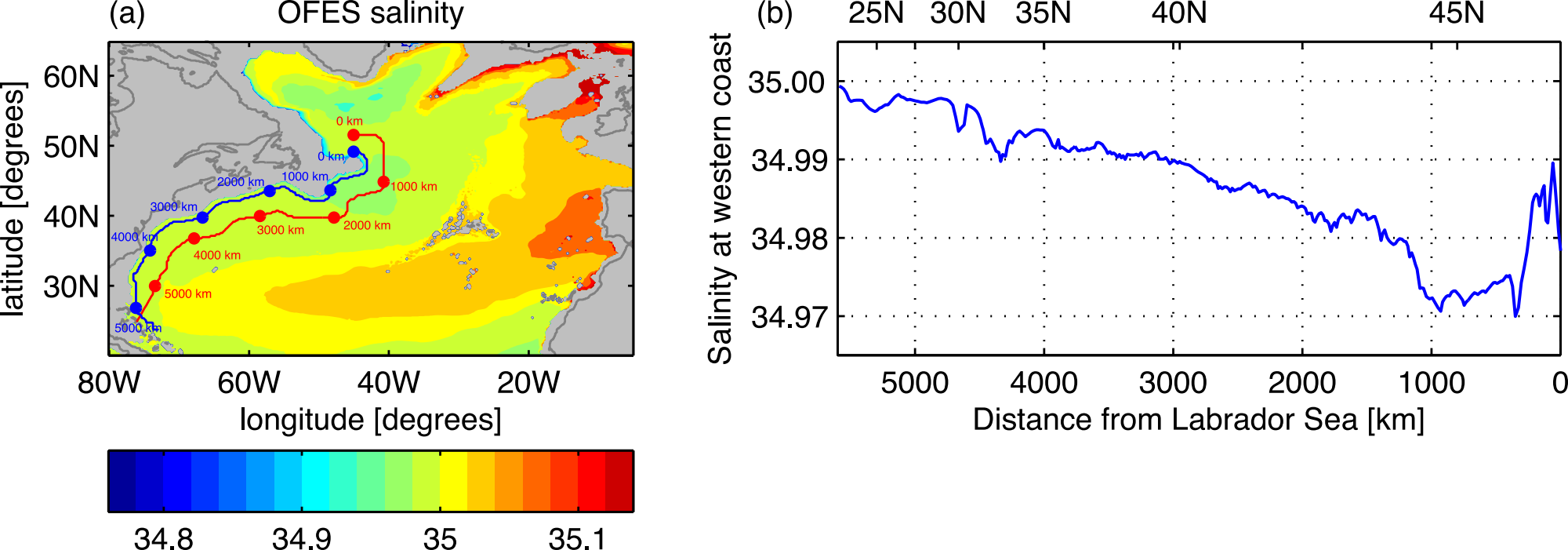
(a)
OFES salinity
60N
50N
40N
30N
latitude [degrees]
80W
60W
40W
20W
longitude [degrees]
0 km
0 km
1000 km
1000 km
2000 km
2000 km
3000 km
3000 km
4000 km
4000 km
5000 km
5000 km
34.8
34.9
35
35.1
(b)
25N
30N
35N
40N
45N
35.00
34.99
34.98
34.97
Salinity at western coast
5000
4000
3000
2000
1000
0
Distance from Labrador Sea [km]

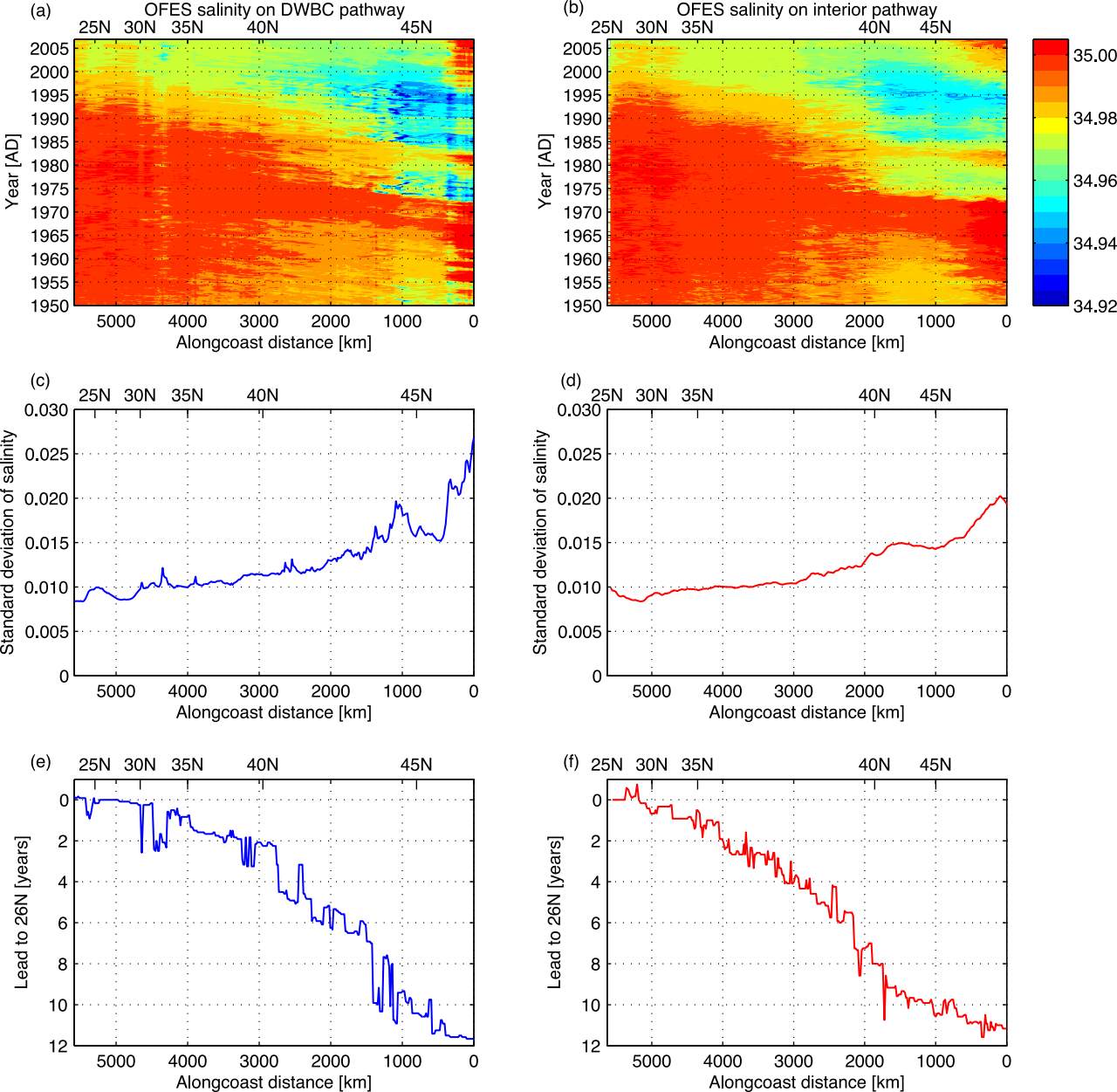
(a)
OFES salinity on DWBC pathway
25N 30N 35N 40N 45N
Year [AD]
2005 2000 1995 1990 1985 1980 1975 1970 1965 1960 1955 1950
5000 4000 3000 2000 1000 0
Alongcoast distance [km]
(b)
OFES salinity on interior pathway
25N 30N 35N 40N 45N
Year [AD]
2005 2000 1995 1990 1985 1980 1975 1970 1965 1960 1955 1950
5000 4000 3000 2000 1000 0
Alongcoast distance [km]
35.00 34.98 34.96 34.94 34.92
(c)
25N 30N 35N 40N 45N
Standard deviation of salinity
0.030 0.025 0.020 0.015 0.010 0.005 0
5000 4000 3000 2000 1000 0
Alongcoast distance [km]
(d)
25N 30N 35N 40N 45N
Standard deviation of salinity
0.030 0.025 0.020 0.015 0.010 0.005 0
5000 4000 3000 2000 1000 0
Alongcoast distance [km]
(e)
25N 30N 35N 40N 45N
Lead to 26N [years]
0 2 4 6 8 10 12
5000 4000 3000 2000 1000 0
Alongcoast distance [km]
(f)
25N 30N 35N 40N 45N
Lead to 26N [years]
0 2 4 6 8 10 12
5000 4000 3000 2000 1000 0
Alongcoast distance [km]

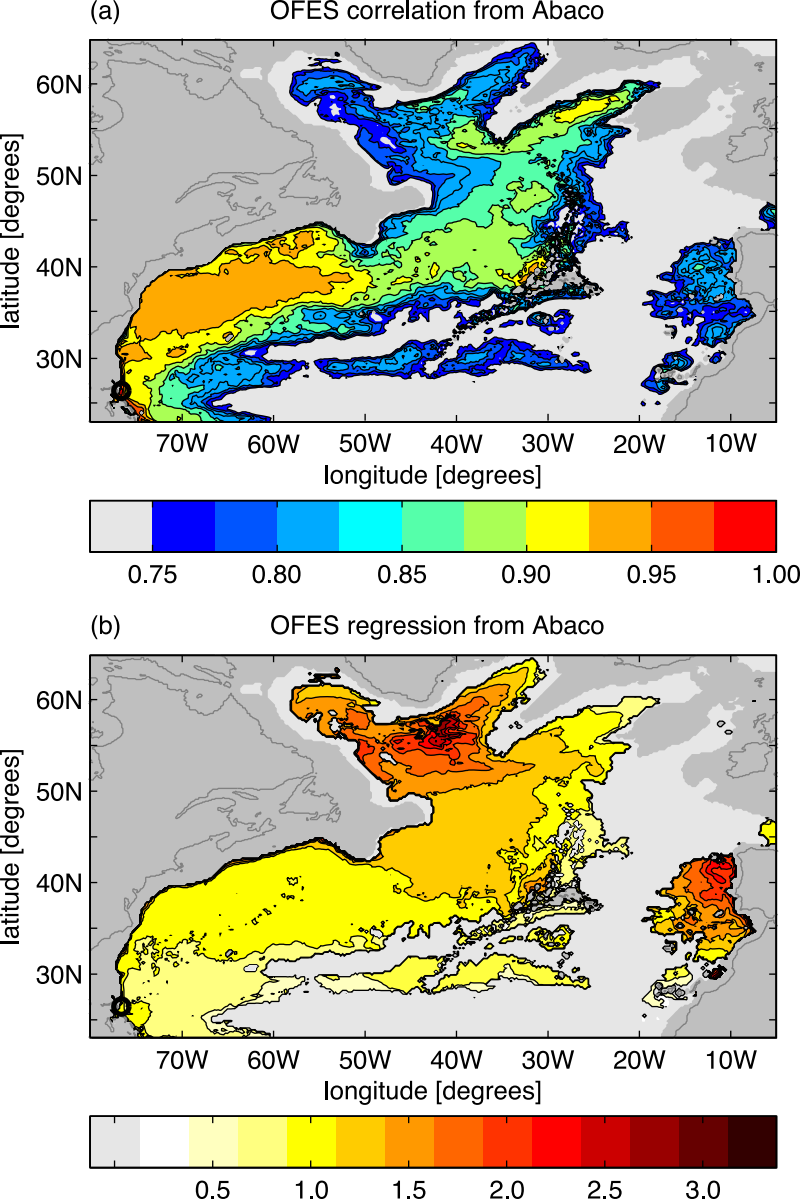
(a)
OFES correlation from Abaco
60N
50N
40N
30N
latitude [degrees]
70W
60W
50W
40W
30W
20W
10W
longitude [degrees]
0.75
0.80
0.85
0.90
0.95
1.00
(b)
OFES regression from Abaco
60N
50N
40N
30N
latitude [degrees]
70W
60W
50W
40W
30W
20W
10W
longitude [degrees]
0.5
1.0
1.5
2.0
2.5
3.0

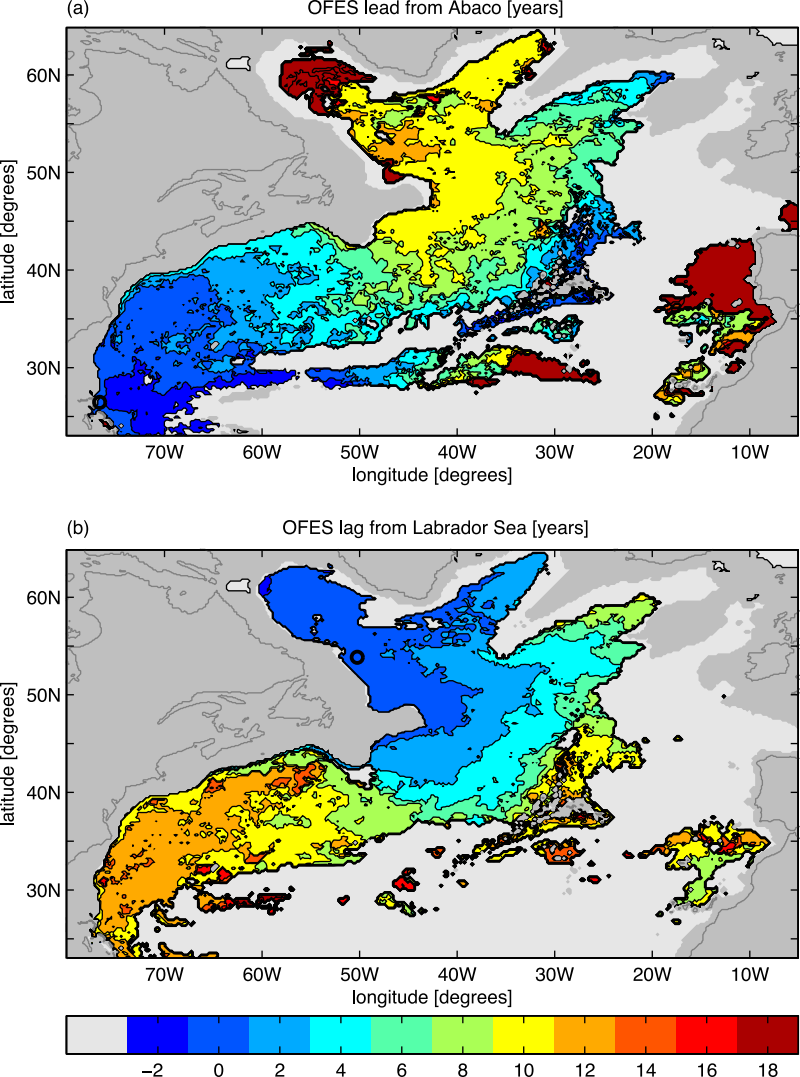
(a)
OFES lead from Abaco [years]
60N
50N
40N
30N
latitude [degrees]
70W
60W
50W
40W
30W
20W
10W
longitude [degrees]
(b)
OFES lag from Labrador Sea [years]
60N
50N
40N
30N
latitude [degrees]
70W
60W
50W
40W
30W
20W
10W
longitude [degrees]
−2
0
2
4
6
8
10
12
14
16
18